

Tracing the Alkinoos Harbor of ancient Kerkyra, Greece, and reconstructing its paleotsunami history

Claudia Finkler¹ | Peter Fischer¹ | Kalliopi Baika² | Diamanto Rigakou³ | Garyfalia Metallinou³ | Hanna Hadler¹ | Andreas Vött¹

¹Institute of Geography, Johannes Gutenberg-Universität Mainz, Mainz, Germany

²Aix-Marseille Université, CNRS, CCJ UMR 7299, Aix-en-Provence, France

³Ephorate of Antiquities of Corfu, Kerkyra, Greece

Correspondence

Claudia Finkler, Institute for Geography, Johannes Gutenberg-Universität Mainz, Johann-Joachim-Becher-Weg 21, 55099 Mainz, Germany.

Email: c.finkler@geo.uni-mainz.de

Scientific editing by Marta Pappalardo

Abstract

In this study, the Alkinoos Harbor of ancient Corfu was investigated by means of geomorphological and sedimentological methods in order to reconstruct the ancient harbor's construction, its period of use and spatial extent, and local paleoenvironmental changes. We present sedimentological evidence for the Alkinoos Harbor that shows distinct signs of dredging activities. Although the harbor must have been in use from the Archaic period onwards, a set of paleoenvironmental proxies based on vibracoring, geophysical prospection, electrical conductivity logging, microfaunal studies, and geochemical analyses revealed typical sediments of a closed, protected Roman harbor that was in use between the 1st and 6th century A.D. In addition, sedimentological and microfaunal evidence allowed us to differentiate between different parts of the Roman harbor. In contrast, the pre-Roman harbor and its shipsheds were built on a sandy seashore. Our data revealed two distinct stratigraphic disruptions related to tsunamigenic impact. These paleotsunamis were dated between the 3rd and 6th century A.D. and between the 5th and 6th century A.D., most probably correlating with the A.D. 365 (Crete) and 6th century A.D. (Peloponnese) supraregional events, respectively. The Alkinoos Harbor turned out to be an outstanding geoarchive to reconstruct human-environment interactions during the late Holocene.

KEYWORDS

geoarchive, harbor geoarchaeology, Ionian Islands, paleotsunami, Roman dredging

1 | INTRODUCTION

The island of Corfu, located in the Ionian archipelago of northwestern Greece (Figure 1A), has a multifaceted history. From the Archaic period onwards (8th to 6th century B.C.), the ancient harbor city of Corcyra (modern Kerkyra = Corfu) emerged as a prevailing sea power in the Mediterranean and took part in the first naval battle ever recorded in Greek history (Thucydides 1.13.4 after Dent, 1910). In the beginning of the Classical period (early 5th century B.C.), it was one of the first Mediterranean city states (polis) to acquire a considerable fleet of triremes and to build adequate harbor and naval installations to accommodate it (Baika, 2003, 2013).

Geoscientific analyses of paleoenvironmental changes through space and time are relevant to better understand the naval status of Corfu, especially in relation to coastal dynamics and the manifold interactions between humans and the local environment. Coastal landscapes are prone to rapid change, and it is therefore important to detect and analyze paleoenvironmental shifts and evaluate how cultures may respond to them. In particular, relative sea level changes,

whether caused by abrupt phenomena like coseismic movements and extreme wave events, or gradual shifts related to climatic oscillations and human impacts are all important triggers for paleoenvironmental change in coastal settings like Corfu.

Unfortunately, geoarchives preserving sedimentary evidence suitable for disentangling the complex history of human-environmental interactions are rare. Ancient harbor deposits are of great interest for geoarchaeological research as they often display excellent preservation due to anoxic and quiescent conditions and are commonly located in cultural centers (Marriner & Morhange, 2007; Morhange, Marriner, & Carayon, 2014). Ancient harbors in the Mediterranean that have been investigated within a framework of interdisciplinary geoarchaeology include those along the coasts of Greece (Fouache et al., 2005; Hadler et al., 2015; Mourtzas, Kissas, & Kolaiti, 2014; Stiros & Blackman, 2014; Vött, 2007; Vött, Schriever, Handl, & Brückner, 2007), Italy (Bini, Chelli, Durante, Gervasini, & Pappalardo, 2009; Di Bella, Bellotti, Frezza, Bergamin, & Carboni, 2011; Goiran et al., 2014; Mazzini, Faranda, Giardini, Giraudi, & Sadori, 2011; Millet, Tronchère, & Goiran, 2014), Turkey (Algan et al., 2009, 2011; Goodman et al., 2009;



FIGURE 1 The ancient city (Palaiopolis) is situated at the eastern shore of Corfu Island (A), adjoining the lake-like Gulf of Corfu in the east. The study site is located on the northern flank of the Analipsis or Kanoni Peninsula, separating the Chalikiopoulou Lagoon (location of the ancient Hyllaikos Harbor) in the west from the Bay of Garitsa (as part of the Gulf of Corfu) in the east (B). Geoarchaeological studies were conducted northwest of the remains of shipsheds (C, D) in the Alkinoos Harbor. Vibracoring sites are marked by black squares, electrical resistivity tomography (ERT) transects by white lines (a–b). The black dashed line marks the boundary between bedrock outcrop (marl) and Holocene coastal and alluvial deposits according to IGME (1970) for the Analipsis Peninsula. Map is based on Bing Aerial 2014, photo by A. Vött, 2012

Kraft, Rapp, Kayan, & Luce, 2003; Seeliger et al., 2013, 2014; Stock, Pint, Horejs, Ladstätter, & Brückner, 2013), France (Bony, Marriner, Morhange, Kaniewski, & Perinçek, 2012; Morhange et al., 2003), and Tunisia (Delile et al., 2015).

Comparable geoarchaeological studies focusing on harbor sediments at Corfu are surprisingly lacking, even though the city was served by two or even three harbor basins, as reported in ancient sources. The Alkinoos Harbor was situated to the north whereas the Hyllaikos Harbor was located to the southwest along the west coast of the Analipsis Peninsula (Figure 1A). These harbors and associated naval infrastructure were developed in order to establish and secure Corfu's supremacy as a naval power in the Mediterranean. Such efforts also reflect the status of the city due to its key strategic position between the Ionian and Adriatic Seas on the trade routes between Greece and Italy (Blackman, 1982; Gehrke & Wirbelauer,

2004; Kiechle, 1979). Both harbors are archaeologically well documented (Baika, 2003, 2013; Dontas, 1965; Kanta-Kitsou, 2001; Lehmann-Hartleben, 1923; Partsch, 1887), although their original topography remains conjectural. The harbors have undergone considerable environmental changes and anthropogenic interventions since antiquity such that their original shape is today partly concealed under modern urban development. Alkinoos Harbor, the focus of the present study, has been completely filled with sediments such that naval installations such as shipsheds of the Classical period lie several hundreds of meters inland today (Baika, 2003, 2013; Dontas, 1966; Preka-Alexandri, 1986).

From a tectonic point of view, the island of Corfu is seismically active, occupying a key position between the tectonically undisturbed shallow Adriatic Sea (Battaglia, Murray, Serpelloni, & Bürgmann, 2004; Maramai, Graziani, & Tinti, 2007) and the Ionian Sea. Located within a

geologically complex system that includes the subduction zone of the Hellenic Arc, continent-continent collisions, and transform fault zones, the area belongs to one of the most seismically active regions in the Mediterranean (Pirazzoli et al., 1994; Sachpazi et al., 2000; van Hinsbergen, van der Meer, Zachariasse, & Meulenkamp, 2006). Traces of seismic and tsunamigenic events that were detected in southern Apulia (Italy), a tectonically stable region, by Mastronuzzi and Sansó (2004), Maramai et al. (2007), and Mastronuzzi, Pignatelli, Sansó, and Selleri (2007) must therefore also have imprinted the sedimentary record of Corfu at the opposite side of the Strait of Otranto near the entrance to the Adriatic Sea.

Ancient harbors can be excellent sediment traps for tsunamis (e.g., Hadler et al., 2013). Furthermore, ancient harbors are usually located in storm-sheltered and quiescent natural positions to protect ships and nearby infrastructure from destructive storm waves. So far, several eastern Mediterranean harbors sites have been analyzed as sediment trap for paleotsunamis, including the Istanbul harbor complex by Bony et al. (2012), the Caesarea harbor by Reinhardt et al. (2006), the Lechaion harbor by Hadler et al. (2013), and the Pheia/Olympia harbor by Vött et al. (2011a).

By means of a multiproxy approach, the present study aims to investigate the geoarchives of the ancient Alkinoos Harbor in order to:

- (i) detect and analyze the sedimentary record of the ancient harbor thus far identified by archaeological evidence;
- (ii) reconstruct the development and use of the harbor in space and time;
- (iii) investigate the paleoenvironmental record of the Alkinoos Harbor basin regarding possible high-energy events such as paleotsunamis.

2 | PHYSICAL AND CULTURAL SETTING

The Ionian archipelago in northwestern Greece is influenced by different tectonic systems. The eastern coasts of the Adriatic Sea are under the influence of continent-continent collision of the Adriatic Microplate toward the Eurasian Plate (Babbucci et al., 2004; Battaglia et al., 2004) and are associated with subsidence and uplift as well as slight deformations (Suric, Korbar, & Juračić, 2014). On Corfu, compressional tectonics drive the Corfu Thrust accompanied by frequent shallow-focus earthquakes (Kokkalas, Xypolias, Koukouvelas, & Doutsos, 2006). In contrast, the southern parts of the Adriatic Sea as well as the Ionian Sea are situated within a seismic stress field between the subduction zones of the Calabrian (southwest) and Hellenic Arc (southeast) (Hollenstein, Müller, Geiger, & Kahle, 2008; van Hinsbergen et al., 2006). These subductions combined with the Kerkyra-Cefalonia depression, the Cefalonia Transform Fault, and several adjoining fault systems strongly affect the geology and form of Corfu Island (Poulos, Lykousis, Collins, Rohling, & Pattiaratchi, 1999). The Ionian Islands therefore show all types of tectonic plate boundaries within a radius of a few hundred kilometers (Sachpazi et al., 2000). Not surprisingly, Corfu is repeatedly listed in earthquake and tsunami catalogues (Abraseys & Synolakis, 2010; Albin, 2004; Hadler,

Willershäuser, Ntageretzis, Henning, & Vött, 2012; Partsch, 1887; Soloviev, Lykousis, Collins, Rohling, & Pattiaratchi, 2000). These entries document several earthquakes with moment magnitude values around 6.0 (Stucchi et al., 2013) on and near the island of Corfu since Medieval times. However, no historical record is available for earlier events (Partsch, 1887).

This gap in historical data must not be interpreted as an absence of earthquakes but is rather related to the incompleteness of the data set (see also Hadler et al., 2012). In fact, on the coasts of Corfu and satellite islands, Evelpidou, Karkani, and Pirazzoli (2014) detected geomorphological indicators of emergence as a result of ancient earthquakes in the form of erosional notches. As already stated by Pirazzoli et al. (1994), these notches document at least two coseismic uplifts for the central and western parts of the island, the first one between the 8th and 4th century B.C., the second one at a later date, so far undated. Similar findings of submerged notches are known from the Croatian coast (Favre et al., 2011; Marriner et al., 2014). Mastronuzzi et al. (2014) even provided geomorphological and sedimentological evidence for a series of tectonic events on Corfu that may be correlated with tsunami impacts reported for comparable time periods from surrounding regions such as Adriatic Italy (Mastronuzzi & Sansó, 2004; Maramai et al., 2007) and Sicily (Barbano, Pirrotta, & Gerardi, 2010; De Martini et al., 2012; Smedile et al., 2011). Concerning tsunamigenic sediments at Corfu itself, Fischer et al. (2016a) present geomorphological and microfaunal evidence of multiple paleotsunamis, traces of which were investigated in coastal lagoons along the southwestern and eastern coasts of the island. Paleotsunami studies were also carried out on the Ionian Islands (Hadler et al., 2011; May et al., 2012; Willershäuser et al., 2013) and the northern Greek mainland (Vött et al., 2010, 2011b).

The ancient city of Corcyra and its harbors are located along the eastern shore of the island (Figure 1A), separated from the Greek mainland and Albania by the Gulf of Corfu, a narrow strait with shallow water depths. Naturally sheltered from the prevailing westerly winds by the curved shape of the island, the gulf features relatively low-energy conditions with maximum water depths of 70 m. Within this sheltered lake-like situation (Partsch, 1887), the ancient city was built on the northern part of the former Analipsis Peninsula (Figure 1B), a ridge of Miocene marls (IGME, 1970) extending up to 60 m above sea level. The ancient city extended northwards into the coastal lowlands of the Bay of Garitsa. The center of the city was located both on top of the Analipsis Peninsula and along its western hillslopes in the narrow strip between the two main harbors, the Alkinoos Harbor to the north, and the Hyllaikos Harbor to the southwest (Figure 1C). It is assumed that the Hyllaikos Harbor was located at the eastern fringe of the modern Chalikiopoulou Lagoon, but the area was strongly transformed by the construction of the modern airport in the 1950s. The location of the Alkinoos Harbor is archaeologically attested by the remains of a series of harbor installations. The name of the harbor originally refers to the Homeric king of the Phaiacians and was adopted by archaeologists (Baika, 2013).

The most impressive harbor remains are those of monumental trireme shipsheds (Kokotou site), constructed in the early 5th century B.C. (Baika, 2003, 2013; Preka-Alexandri, 1986; Spetsieri-Choremi, 1996). The shipsheds consist of rows of piers out of local white

limestone, running southeast-northwest toward the presumed ancient coastline (Figure 1C and D; cf. Baika, 2013). This shipshed complex is located in close proximity to the ancient agora of the city and most probably belongs to the harbor installations as also referred to incidentally by ancient sources (Baika, 2013, 2015; Thucydides 3.72.3 after Dent, 1910). In the Roman period, the area was rearranged and overbuilt. As a result, remains of the Roman agora pavement can now be seen to the southwest of the shipshed complex (Figure 1C). Furthermore, a section of a quay wall, interrupted by slipways and showing a different, namely south-north orientation, was excavated to the east of the Kokotou shipsheds naval zone (Baika, 2013; Riginos, Karamanou, Kanta, Metallinou, & Zernioti, 2000; Figure 1C). Although it is still uncertain whether all these harbor facilities belong to one and the same Alkinoos Harbor, the quay wall remains clearly demonstrate the existence of a harbor installation facing the Bay of Garitsa. Systematic geoarchaeological studies are needed concerning the structure and sediment fill of the Alkinoos Harbor and other harbor settings of the ancient city. A third harbor basin is mentioned in historical sources, but not yet located as archaeological and geological evidence is still missing (Baika, 2003; Lehmann-Hartleben, 1923; Partsch, 1887; Riginos et al., 2000).

3 | METHODS

The study area within the ancient Alkinoos Harbor (Figure 1C) was investigated using a multimethodological approach. Vibracoring was conducted using engine-driven devices (Nordmeyer RS 0/2.3 drill rig and Atlas Copco Cobra mk 1) with core diameters of 50–80 mm to investigate the sedimentological record of the assumed harbor basin. Vibracores were cleaned, photographed, and described in the field (ad Hoc-Arbeitsgruppe Boden, 2005; Schrott, 2015). Selected vibracores (suffix "A": KOR 1A, KOR 6A, and KOR 24A; for location see Figure 1C) were drilled using closed auger heads with enclosed plastic liners to enable *in situ* measurements in the laboratory.

On-site geoelectrical prospecting allowed for identification of subsurface stratigraphy and archaeological structures due to variable electrical resistivity owing to differences in grain-size, mineral composition, water content, and pore structure (Keary, Brooks, & Hill, 2002). We conducted electrical resistivity tomography (ERT) using a multi-electrode device type Syscal R1+ Switch 48 (Iris Instruments) and a Wenner–Schlumberger electrode array. Data were processed by means of the RES2DINV Software and least-squares inversion (Loke, Acworth, & Dahlin, 2003; Loke & Dahlin, 2002). Elevation and position data of vibracoring sites and ERT locations were measured by means of a differential GPS (Topcon HiPer Pro).

In situ Direct Push electrical conductivity (EC) measurements turned out to be a valuable tool to trace grain-size fluctuations with a high resolution, mirroring changes in the depositional environment (Fischer et al., 2016b). EC logging was realized at selected vibracoring sites using a Geoprobe SC520 device. The probe consists of four electrodes in a linear arrangement. By using a Wenner electrode array the electrical conductivity as well as the rate of penetration were

measured at a high resolution of 0.2 cm (see also Harrington & Hendry, 2006; Schulmeister et al., 2003).

In the laboratory, X-ray fluorescence (XRF) analyses were accomplished by means of a handheld Niton XL3t 900S GOLDD (calibration mode SOIL) to determine the concentrations of more than 30 elements that were used to trace geochemical fingerprints of different environmental settings. If possible, these measurements were conducted *in situ* at the sediment-filled liners with an average resolution of 2 cm or otherwise at selected samples. Additionally, we analyzed grain-size classes after the Köhn pipette method and measured loss on ignition (LOI) as an indicator for the concentration of organic material (Blume, Stahr, & Leinweber, 2011).

The microfaunal contents of selected vibracores (KOR 1A, KOR 5) were analyzed by means of a semiquantitative screening. For this purpose, 15 ml of sediment were extracted from selected stratigraphic layers and sieved in fractions of >400 μm , >200 μm , >125 μm , and <125 μm . Species were determined after Loeblich and Tappan (1988) and Cimerman and Langer (1991) using a stereomicroscope. Additionally, photos of selected specimens were taken using a scanning electron microscope (SEM). Species were classified according to their ecological habitat preferences after Murray (2006) and Sen Gupta (1999). The determination of microfaunal remains helps to reconstruct environmental conditions and to detect allochthonous interferences (Dominey-Howes, Cundy, & Croudace, 2000; Hadler et al., 2013; Mamo, Strotz, & Dominey-Howes, 2009; Willershäuser et al., 2013) as progressive environmental changes will result in gradually shifting microfaunal assemblages, while abrupt changes will either severely stress or kill the preexisting fauna, the latter visible in a sudden shift of species. We further calculated a simplified index considering the number of species (diversity) and the total amount of specimens (grouped abundance) to better visualize these shifts. We focused on foraminiferal fingerprints, as foraminifera commonly occur under various conditions and throughout the record (Sen Gupta, 1999; Murray, 2006).

A local geochronostratigraphy was established by means of ^{14}C accelerator mass spectrometry (AMS) dating of nine selected organic samples (Table I) performed by the Klaus-Tschira Laboratory of the Curt-Engelhorn-Centre Archaeometry gGmbH Mannheim (MAMS), Germany, and by the Keck Carbon Cycle AMS Facility (UCI), University of California at Irvine, USA.

4 | RESULTS: DECIPHERING THE GEOARCHIVE OF THE ANCIENT HARBOR

Six vibracores were drilled along two transects where archaeological remains of harbor installations suggest the possible location of the ancient Alkinoos Harbor basin (Figure 1B and C; see also above). More specifically, the harbor basin is related to the trireme shipshed complex (Kokotou site) dating to the early 5th century B.C., excavated at the northern fringe of the Analipsis Peninsula. In general, shipsheds were functional structures to accommodate and protect warships. They were built as roofed galleries perpendicular to the coastline and in inclination toward the sea, so that warships could be

TABLE I Radiocarbon dates from the Alkinoos Harbor area

Sample ID	Depth (m b.s.)	Depth (m b.s.l.)	Sample Material	Lab. No.	$\delta^{13}\text{C}$ (ppm)	^{14}C Age (yr B.P.)	2σ Age (B.C./A.D.)	1σ Age (B.C./A.D.)
KOR 1A/6+ HK	2.22	0.56	Charcoal	UCI 121508	^a	1560 ± 25	A.D. 424–554	A.D. 430–541
KOR 1A/9+ HK	2.65	0.99	Charcoal	UCI 121509	^a	1600 ± 25	A.D. 404–536	A.D. 413–533
KOR 1A/21+ PR	4.12	2.46	Unidentified plant remains	UCI 121510	^a	1770 ± 25	A.D. 143–342	A.D. 236–325
KOR 1A/24+ HR	4.65	2.99	Wood fragment	UCI 121511	^a	1895 ± 25	A.D. 55–211	A.D. 78–177
KOR 5/14 PR	4.19	2.89	Seaweed	MAMS 19768	−14.1 ^b	2200 ± 22	A.D. 81–235	A.D. 104–188
KOR 5/25+ HR2	8.27	6.97	Wood fragment	MAMS 19769	−23.5	7199 ± 28	6198–6003 B.C.	6069–6026 B.C.
KOR 5/32+ HR	9.81	8.51	Unidentified plant remains	MAMS 19770	−27.4	7328 ± 28	6238–6089 B.C.	6232–6104 B.C.
KOR 25/13 HR	3.47	2.89	Wood fragment	MAMS 19778	−29.0	1729 ± 19	A.D. 251–381	A.D. 256–343
KOR 25/27+ PR	6.36	5.78	Unidentified plant remains	MAMS 19779	−30.3	7022 ± 27	5984–5846 B.C.	5979–5887 B.C.

Note: b.s., below ground surface; b.s.l., below sea level; Lab. No., laboratory number; Klaus-Tschira Laboratory of the Curt-Engelhorn-Centre Archaeometry gGmbH Mannheim, Germany (MAMS), and Keck Carbon Cycle AMS Facility, University of California at Irvine, USA (UCI); $1\sigma/2\sigma$ age, calibrated ages, $1\sigma/2\sigma$ range. All dates are calibrated using the IntCal13/Marine13 curve by Calib 7.0 (Reimer et al., 2013; Stuiver & Reimer, 1993).

^a ^{13}C correction is done automatically with a standard run.

^b Marine sample, calibrated by using the marine calibration data set with an average reservoir age of 405 years.

rapidly launched and hauled out of the water (Blackman, Rankov, Baika, Gerding, & Pakkanen, 2013). Therefore, in the Kokotou site, based on the shipsheds' orientation and its relationship to the presumed ancient coastline needed for the shipsheds to be operational, the harbor basin is assumed to be located directly in front of the recovered rows of piers toward the northwest. This hypothesis is further supported by the discovery of associated harbor facilities. These include the eastern entrance tower of the harbor located to the north of the study site, as well as another shipshed complex (Dontas, 1966) located farther northwest of the Kokotou site (for further details see Baika, 2013, 2015).

Vibracoring sites KOR 1A and KOR 2 are located close to the excavated shipsheds (Figure 1D), approximately 200 m from the present coastline. Vibracore KOR 1A was drilled some 50 m and vibracore KOR 2 some 20 m to the north of the shipshed remains. While vibracoring site KOR 2 is located near the wall remains of a Roman installation, another wall structure was encountered between both vibracoring sites. Vibracore KOR 6A is located some 10 m to the west of the shipshed remains. It was drilled on a higher level right next to the remains of the Roman agora pavement. In contrast, Transect II comprises vibracores KOR 5, KOR 25, and KOR 24A and covers the western part of the presumed ancient harbor zone lying about 150 m to the northwest of the Kokotou shipshed remains (see Figure 1C).

Vibracore Transects I and II provide valuable insight into the local stratigraphic record (Figure 2): Bedrock was only found in the eastern part of Transect I and is composed of Miocene marl (Unit 1, IGME, 1970). The western part of Transect II revealed gray clayey to silty lagoonal deposits (Unit 2) dated to the Mid-Holocene. Thereafter, a long period of stable shallow marine conditions (Unit 3) obviously lasted until ancient times. Toward the north, lagoonal sediments are alternating with shallow marine fine sand (KOR 5). In the most western part of the study area along Transect I, this marine sand unit directly covers the Miocene bedrock. Several coarse sand layers

including marine shell debris within this unit were found at sites KOR 6A, KOR 25, and KOR 24A. Toward the east, Unit 3 is followed by dark gray to dark brown clayey silts representing the (re)establishment of lagoonal conditions (Unit 4). At site KOR 1A, this unit is again interrupted twice by coarse sand containing shell debris and ceramics. In contrast, Unit 4 is missing at sites KOR 2 and KOR 6A where the fine sand is covered by heterogeneous debris containing ceramics and bricks within a silt matrix (Unit 6). In the western part of Transect II, Unit 4 is followed by clayey silt of light gray color (unit 5) containing several intersecting dark gray to black peat-like organic layers that document semiterrestrial conditions.

4.1 | Stratigraphic record at the shipsheds site (Transect I)

Figure 3 depicts depositional facies found at vibracoring site KOR 1A. Miocene marl is covered by shallow marine fine sand, which in turn is overlain by dark gray lagoonal mud. On top, we found anthropogenic fill containing bricks, ceramics, and debris. Within and on top of the lagoonal deposits, two abrupt coarse-grained layers were encountered. These layers are also documented in Figure 4, where selected multiproxy data for vibracores KOR 1A and KOR 2 are illustrated.

The grain-size distribution of vibracore KOR 1A allows one to differentiate between distinct sedimentary units. Miocene bedrock is dominated by clay and silt, whereas overlying shallow marine deposits are characterized by high amounts of finest sand and fine sand. Lagoonal sediments, however, are dominated by clay and silt with low amounts of sand. Sand layers intersecting the lagoonal mud show abrupt changes in grain-size distribution with multiple peaks within the sand fraction and high contents of skeletal components. LOI values are constantly high in lagoonal deposits reaching maximum values in the very upper part of this unit (Figure 4). EC values are consistently low (around 40 mS/m) for shallow marine sand deposits. In contrast, EC values clearly increase for the coarse-grained material intersecting

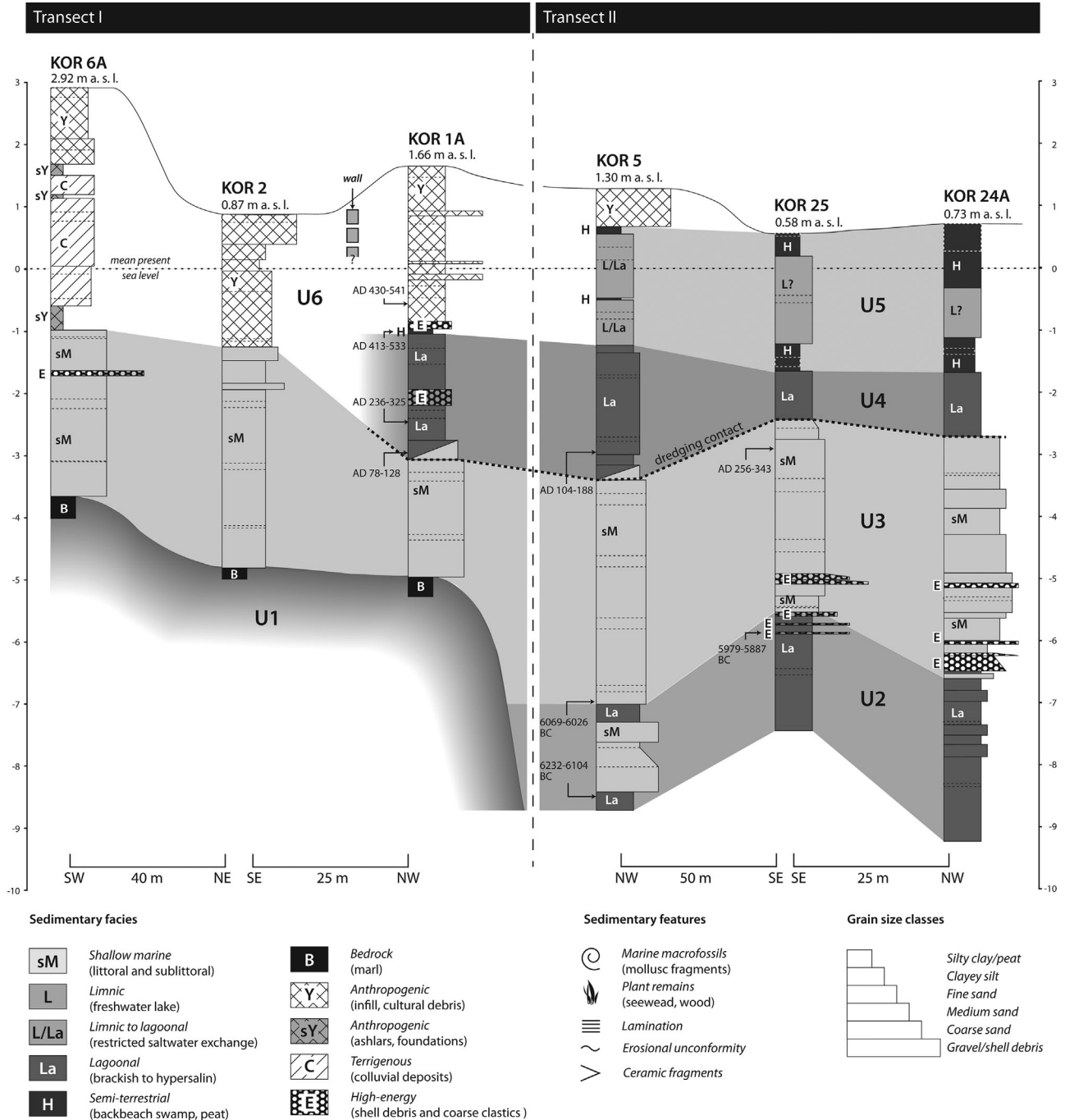


FIGURE 2 Simplified facies patterns found for vibracore Transects I (left) and II (right). For location of vibracoring sites see Figure 1. All radiocarbon ages are calibrated at 1σ (see Table 1)

lagoon-type deposits. Within anthropogenic units, EC values are strongly fluctuating. Differences in the EC log are due to differences in grain and pore size distributions and differences in the mineral composition (Schulmeister et al., 2003). Increasing lead (Pb) concentrations appear with the onset of lagoonal conditions while the lower half of the core is void of Pb. Maximum Pb concentrations were found within the anthropogenic fill on top.

In contrast to KOR 1A, the stratigraphic record of vibracore KOR 2 does not contain a lagoonal sedimentary unit. Sand-dominated shallow marine deposits on top of bedrock material are directly covered by cultural debris. Grain-size distribution, however, reveals a distinct

peak of coarse silt and fine sand in the shallow marine deposits toward the base of the anthropogenic fill. EC values are high within the bedrock but constantly low to medium in the shallow marine sand unit.

Microfaunal analyses (Figure 5) of selected samples of vibracore KOR 1A yielded distinct paleoenvironmental characteristics associated with the different sediment facies. Foraminifera found in the Miocene bedrock such as planktonic foraminifera, *Ammonia beccarii*, *Elphidium* sp., and *Uvigerina* sp. are also ubiquitous in other layers and are therefore considered as geogenic background signal. In addition, the marl contains some cold marine species from the shelf

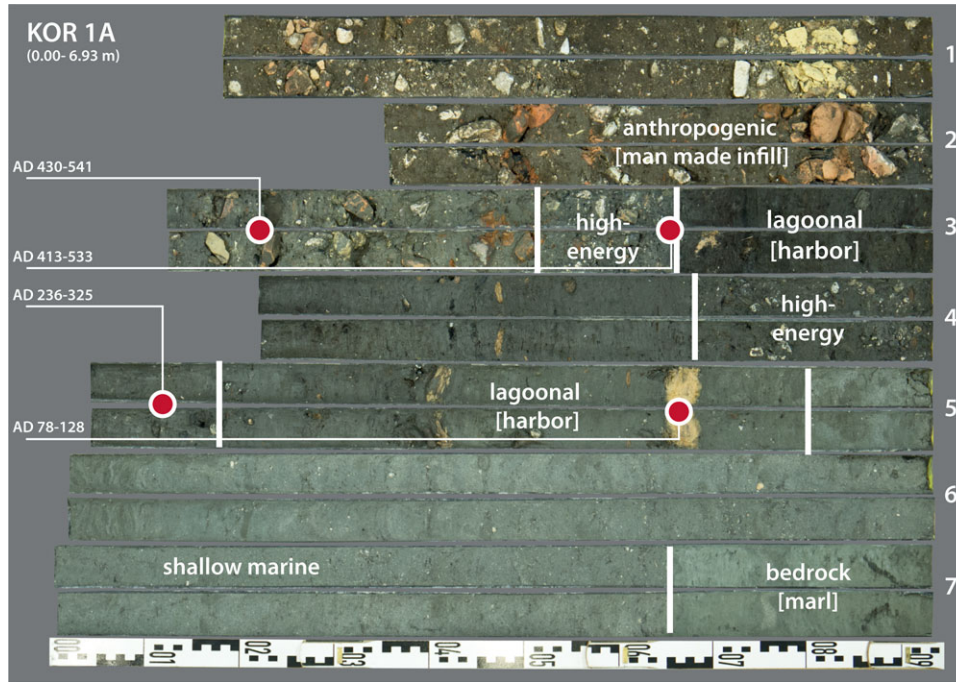


FIGURE 3 Photo of vibracore KOR 1A with the main stratigraphic units and radiocarbon ages (red circles; ages are 1σ values calibrated with Calib 7.0, see Table I). For location of vibracoring site see Figure 1. Note the fine-grained, organic-rich lagoonal deposits, representing a harbor lagoon, which are interrupted and followed by coarse-grained high-energy layers

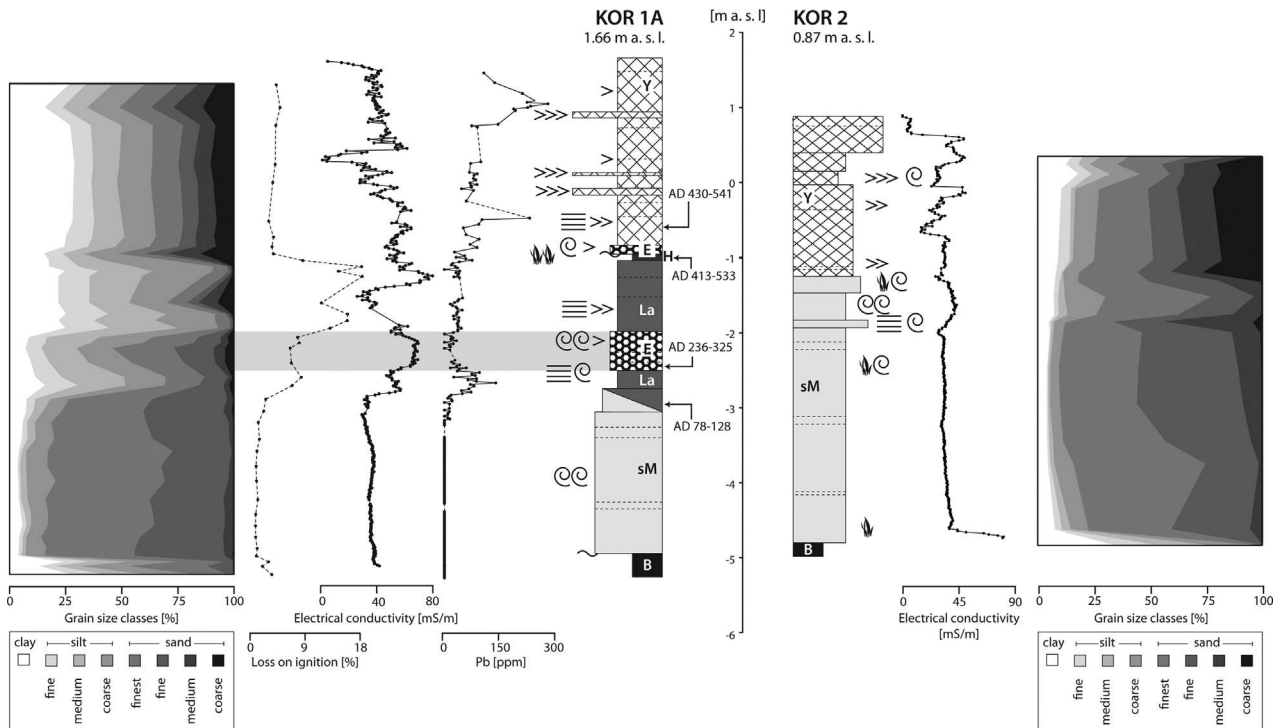


FIGURE 4 Results of multiproxy analyses of vibracores retrieved from the Alkinoos Harbor showing facies classifications, sedimentary features, electrical conductivity, selected geochemical parameters, and grain-size data of vibracores KOR 1A (left) and KOR 2 (right). For location of vibracoring sites see Figure 1; legend according to Figure 2; see text for further explanation

to bathyal region like *Brizalina* sp. or *Lenticulina* sp. (Murray, 2006). Shallow marine deposits, on the other hand, provide a distinct environmental signal and are characterized by high diversity and high abundance resulting in high microfauna index values. Many species, especially Miliolidae (e.g., *Quinqueloculia* sp., *Triloculia* sp., *Sigmoilinita*

costata) appear solely in this environment. Additionally, typical inhabitants of seaweed meadows were found such as *Rosalina* sp. and *Elphidium macellum*. Within the lagoonal sediments, the microfaunal assemblage shifts abruptly toward very low abundance and diversity (Figure 5). Only a few species such as *Ammonia tepida* and *Gyroidina*

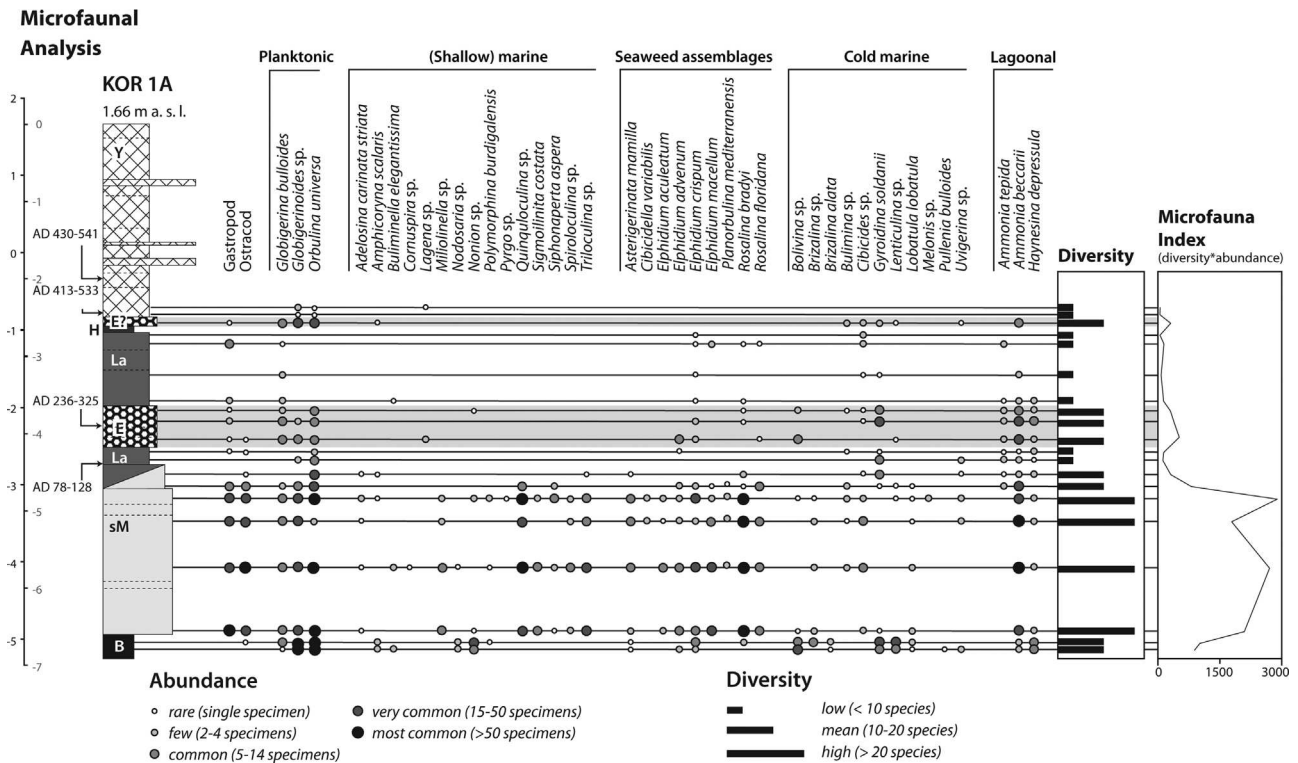


FIGURE 5 Results of microfaunal studies of selected samples from vibracore KOR 1A. For location of vibracoring site see Figure 1; for explanations see text and Figure 2. Foraminifera were determined after Loeblich and Tappan (1988) and Cimerman and Langer (1991) and are classified according to their ecological preferences after Murray (2006) and Sen Gupta (1999). Note the difference in abundance, diversity, and species between the autochthonous lagoonal deposits and the intersecting high-energy layers

sp. are obviously able to inhabit this environment. In contrast, the sand layers intersecting the lagoonal unit again show higher abundance and diversity, visible in distinct peaks within the microfaunal index. In addition to the species appearing in the lagoonal sediments, these sand layers also contain *Bolivina* sp., *Lenticulina* sp., *Amphicoryna scalaris*, and *Lagena* sp.

4.2 | Sedimentary record of the western harbor area (Transect II)

Vibracore transect II was drilled in the western part of the study area (Figure 1). Figure 6 shows selected multiproxy parameters of vibracore KOR 5. Clayey silt in the lower part of the core, representing lagoonal conditions, is covered by homogenous shallow marine sand mostly consisting of finest and fine sand. At 3.38 m below sea level (b.s.l.), the sand is overlain by clay- and silt-dominated lagoonal mud. This in turn is overlain by limnic to lagoonal clayey silt.

The concentration of Pb is subject to strong fluctuations within the core. While the values vary on a low level in the shallow marine sand unit, the Pb content reaches maximum values within lagoonal deposits. LOI values are uniformly low with only the lower and upper sections of the lagoonal deposits showing values greater than 10%. The lower lagoonal unit contains high iron (Fe) but relatively low calcium (Ca) concentrations, resulting in a low Ca/Fe ratio, while the overlying marine sand shows increasing Ca values and constantly low Fe concentrations. Within the upper lagoonal unit, the Ca/Fe ratio is higher compared to

the lower lagoonal unit, most probably associated with higher amounts of finest sand. Lagoonal sediments on top are characterized by a low Ca/Fe level.

Results of microfaunal analyses conducted for selected samples from core KOR 5 are depicted in Figure 7. Comparable to KOR 1A, some species are ubiquitous and seem to represent the geogenic background signal. Lagoonal mud from the base of the core, however, is characterized by low abundance of some species such as *Rosalina floridana*, *Planorbulina mediterraneensis*, and *Adelosina carinata-striata*. In contrast, the subsequent shallow marine sand shows a significantly high microfauna index due to large numbers of Miliolidae like *Triloculina* sp. or *Miliolinella subrotunda*, typical seaweed meadows inhabitants such as *Rosalina bradyi* or *Elphidium* sp. (Murray, 2006) and species solely appearing in this (sub)littoral environment like *Gyroidina soldanii*. With the establishment of the following upper lagoonal unit, new species occur with decreasing abundance and diversity toward the top, namely Miliolidae, *Rosalina floridana*, *Elphidium advenum*, *Rosalina bradyi*, and *Globigerina bulloides*. A further shift in the foraminiferal remains documents a clear change with strongly restricted saltwater exchange in the lagoonal environment documented by only few saltwater species such as *Amphicoryna scalaris* and *Lenticulina* sp. but increasing numbers of ostracods.

Vibracores KOR 25 and KOR 24A show minor differences regarding their sedimentary records compared to vibracore KOR 5. Grain-size data reveal a clear dominance of clay and silt within the lower lagoonal unit of core KOR 25, intercalated with several sand layers including

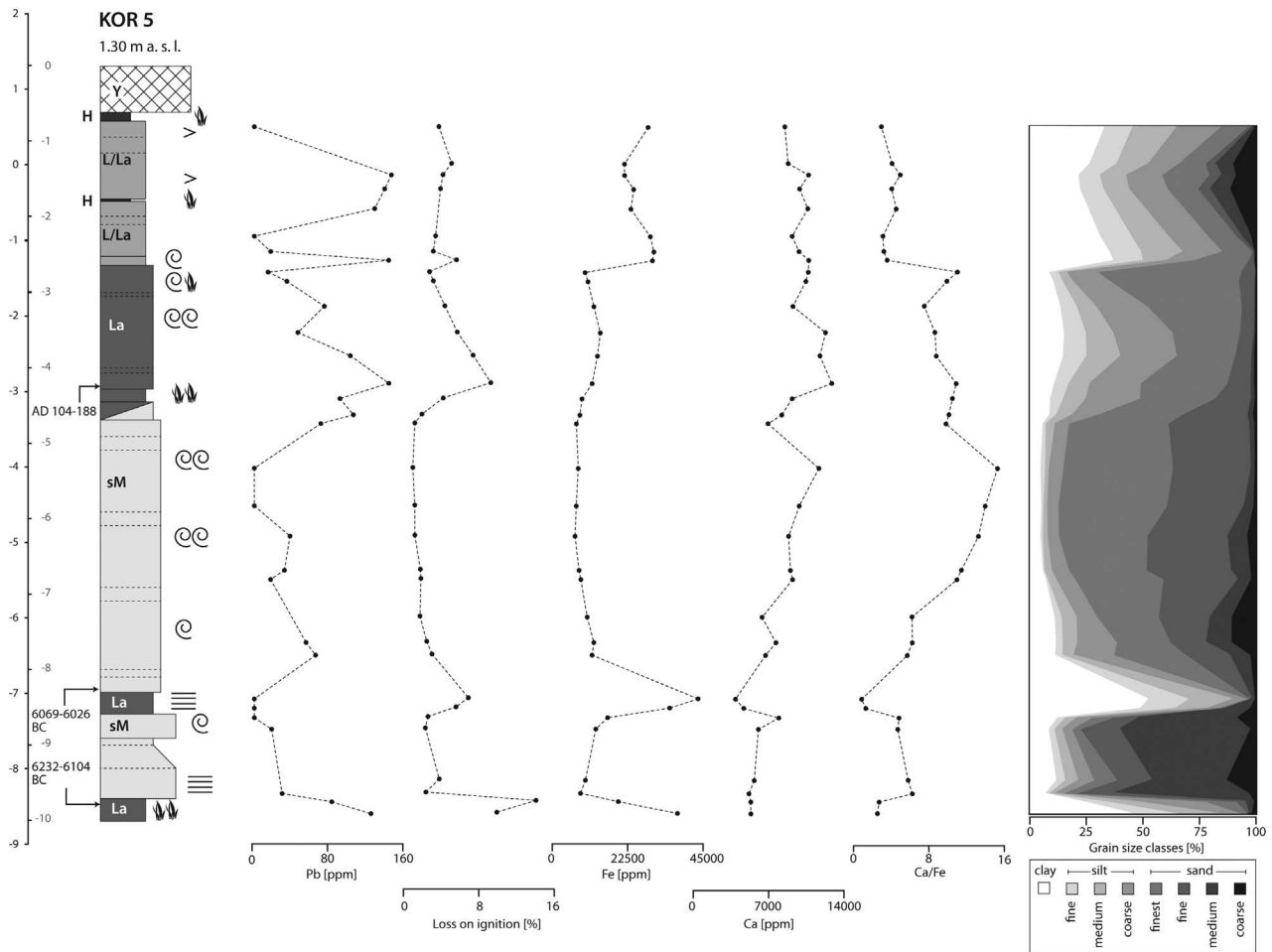


FIGURE 6 Sedimentary units and features, grain-size data, and selected geochemical parameters of vibracore KOR 5 from the western part of the Alkinoos Harbor basin. For location of vibracoring site see Figure 1, for explanations see text; legend according to Figure 2

considerable amounts of medium and coarse sand (Figure 8). In contrast, the subsequent thick unit of shallow marine sand is mostly made out of finest and fine sand. The overlying lagoonal unit is characterized by silt with only minor amounts of clay, especially when compared to the lower lagoonal unit and the limnic sediments in the upper part of the core. The latter consist of nearly equal amounts of clay and silt while sand is almost missing.

The concentration of Pb shows very similar patterns for vibracores KOR 24A and KOR 25. A distinct rise in Pb is observed with the onset of lagoonal sediments at approximately 2.40 m b.s.l. (Figure 8). Highest values are reached within semiterrestrial peat-like deposits in the upper parts of the cores. LOI values increase in lagoonal mud and reach their maximum within the peat-like sediments.

4.3 | Results from electrical resistivity tomography

Electrical resistivity tomography (ERT) measurements were conducted along several transects at the Alkinoos Harbor site. Combining ERT and vibracoring stratigraphies, we obtained 2D and 3D information on the extent of specific layers. Figure 9 shows the results of ERT transects KOR ERT 16 and 78.

Transect KOR ERT 16 (Figure 9A) was conducted right in front of the excavated shipsheds between vibracoring sites KOR 1 and KOR 6A. The ERT depth section shows a sequence of low electrical resistivity values ($<20 \Omega\text{m}$; green/blue) at the base and high values toward the top. Whereas the lower unit appears to be very homogeneous, the upper surface-near unit includes clearly delimited structures with electrical resistivity values up to $80 \Omega\text{m}$. Four structures in the eastern part of the section were found for the same depth level at ~ 0.5 m above sea level, while other structures toward the west are located on a lower level at approximately present sea level. Also, an underlying section of lower resistivity dips in a step-like manner.

ERT results of transect KOR ERT 78 (Figure 9B) reveal a more heterogeneous distribution of electrical resistivity. The southeastern part of the transect shows uniform values $<7 \Omega\text{m}$, only material near the surface appears to be slightly more resistant. This distribution in electrical resistivity fits well with the stratigraphy of vibracore KOR 25 where shallow marine sands are followed by lagoonal deposits. Northwest of transect KOR ERT 78, the upper part of the depth section shows a high-resistivity layer reaching values up to $22 \Omega\text{m}$. A distinct shift in electrical resistivity is marked by a sharp contact to the unit below where electrical resistivity reaches approximately $10 \Omega\text{m}$. Note the step-like contour of this unit in Figure 9.

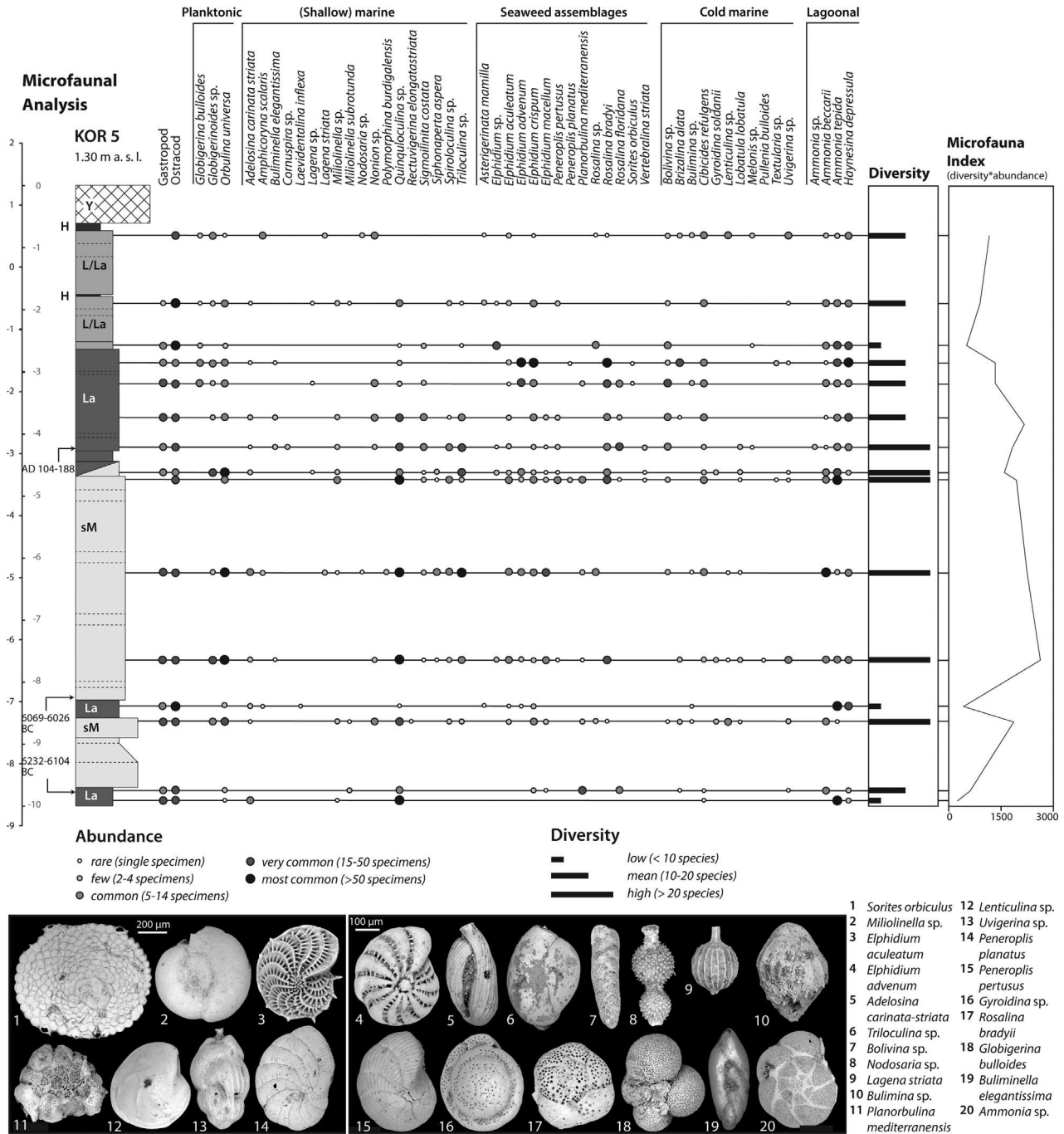


FIGURE 7 Results of microfaunal studies of selected samples from vibracore KOR 5. For location of vibracoring site see Figure 1; for explanations see text; legend according to Figure 2. Photos of selected samples were taken using a scanning electron microscope (SEM). Foraminifera species were determined after Loeblich and Tappan (1988) and Cimerman and Langer (1991) and are classified according to their ecological preferences after Murray (2006) and Sen Gupta (1999). Note the different foraminiferal fingerprint of the upper lagoonal unit (high diversity, high abundance) compared to the lower lagoonal deposits that are characterized by a distinctly lower abundance and diversity

4.4 | Dating approach

Nine samples consisting of charcoal and plant remains were selected for ¹⁴C AMS dating and calibrated with the IntCal13 curve using software Calib 7.0 (Stuiver & Reimer, 1993, Reimer et al., 2013; Table I). According to the relatively high δ¹³C value of -14.1 ‰, sample KOR 5/14 PR suggests a marine origin (Walker, 2005) and was calibrated using the Marine13 curve. A local marine reservoir curve for Corfu

does not exist. Local variations of the reservoir effect for different types of organic material as well as different depositional environments are still unknown. Therefore, we used a mean global reservoir correction of 405 years within this study (Reimer et al., 2013). However, this correlates well with the reservoir ages estimated for the western Mediterranean, for Zante, and the eastern Adriatic Sea to be around 400 years, 439 years, and 421 years, respectively (Siani et al., 2000, Reimer & McCormac, 2002).

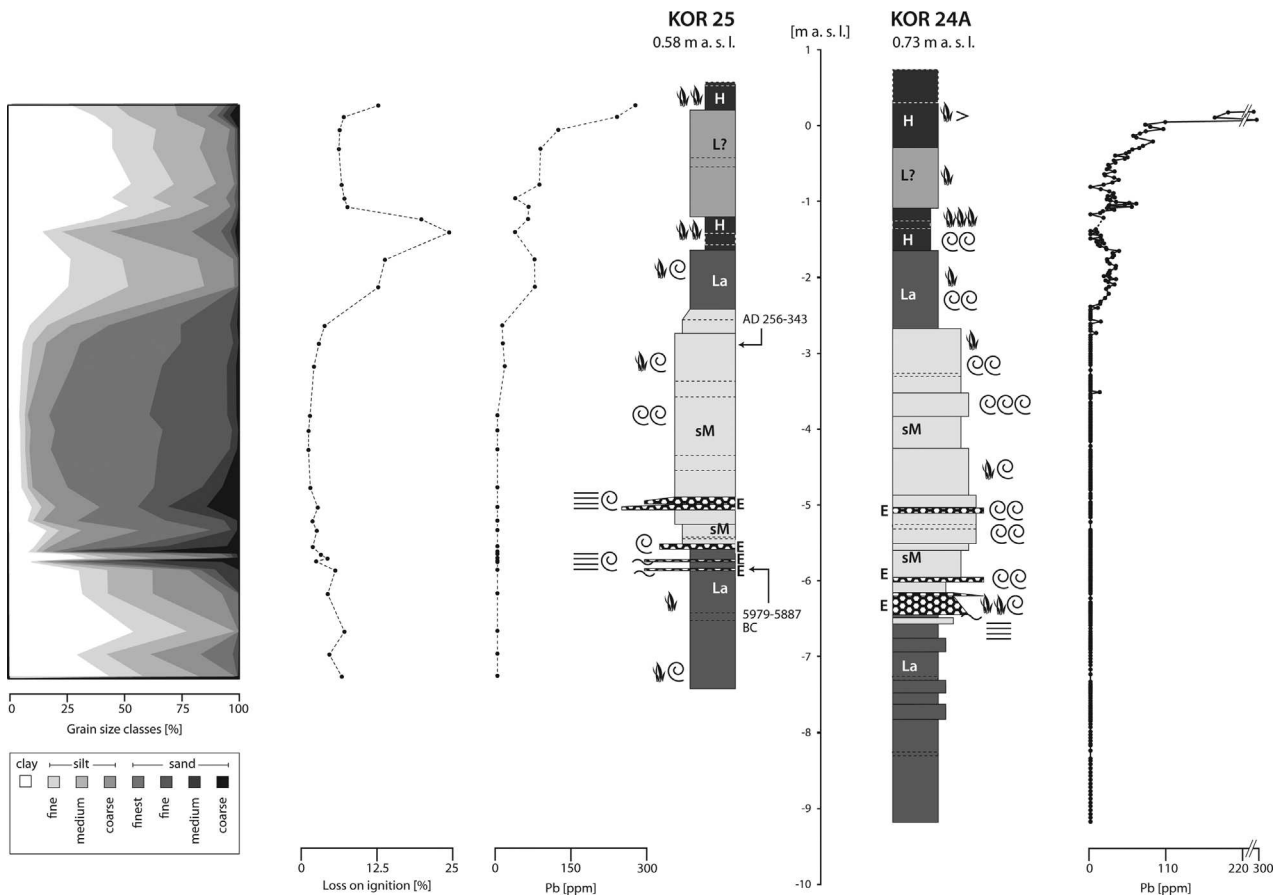


FIGURE 8 Facies classification, sedimentary features, selected geochemical parameters, and grain-size data of vibracores KOR 25 (left) and KOR 24A (right). For location of vibracoring sites see Figure 1; for explanations see text; legend according to Figure 2. Pb content of vibracore KOR 24A (right) was measured *in situ* with an average resolution of 2 cm, while Pb content of vibracore KOR 25 (left) was measured with lower resolution at selected samples. In contrast to the lower lagoonal unit, the upper lagoonal mud shows distinct peaks in anthropogenic Pb content associated with high values in LOI

Generally, ^{14}C results should be regarded as approximate time-frames rather than as fixed dates, because contamination or relocation of carbon, isotopic fractionation, local marine reservoir, or hard water effects as well as long-term variations with ^{14}C production may occur (Walker, 2005). Moreover, dating high energy layers by means of radiocarbon dating is problematic due to reworking effects (Vött et al., 2009). For this reason, where possible, we retrieved samples from the over- and underlying deposits. By this “sandwich” dating approach, a time window is framed by a *terminus post quem* (before the event) and a *terminus ante quem* (after the event) and provides time frames for the different stratigraphic layers for both vibracore transects (Figure 2). Ages presented in Table 1 and Figure 2 do not contain age inversions and are therefore considered reliable.

5 | DISCUSSION

5.1 | Ancient harbor sediments

Based on our multiproxy geoarchaeological approach it was possible, for the first time, to obtain physical evidence for the development of Alkinoos Harbor that complements archaeological evidence such as the excavated remains of shipsheds (Baika, 2003, 2013;

Dontas, 1966) as well as historical records (e.g., Thucydides 3.72.3 after Dent, 1910) indicating the broad position of the harbor basin. Geophysical studies conducted close to the shipsheds (Figure 9) revealed several highly resistant structures, clearly delimited from the surrounding material. These structures are located in the direct alignment of the excavated shipsheds such that we are tempted to interpret them as a continuation of the shipsheds rows of piers, still uncovered, in a northwestern direction. However, this zone was rearranged in Roman times, as documented by extensive Roman installations that were excavated directly on the presumed northwestern alignment of the shipsheds. Further archaeological excavation and stratigraphic surveys are, however, needed for validation. In any case, these wall remains, so far unknown, appear to be founded on a unit with low electrical resistivity, which, according to vibracores KOR 6A and KOR 2, corresponds to fine sand deposited in a shallow marine environment. These conditions must have been established after ca. 6000 B.C. and persisted until ancient times.

Vibracores KOR 1A, KOR 5, KOR 25, and KOR 24A show lagoonal mud overlying this shallow marine sand unit. The predominant grain-size is clayey silt indicating quiescent environmental conditions, well protected from beach dynamics. Electrical conductivity is higher within lagoonal deposits compared to shallow marine sand. LOI values are

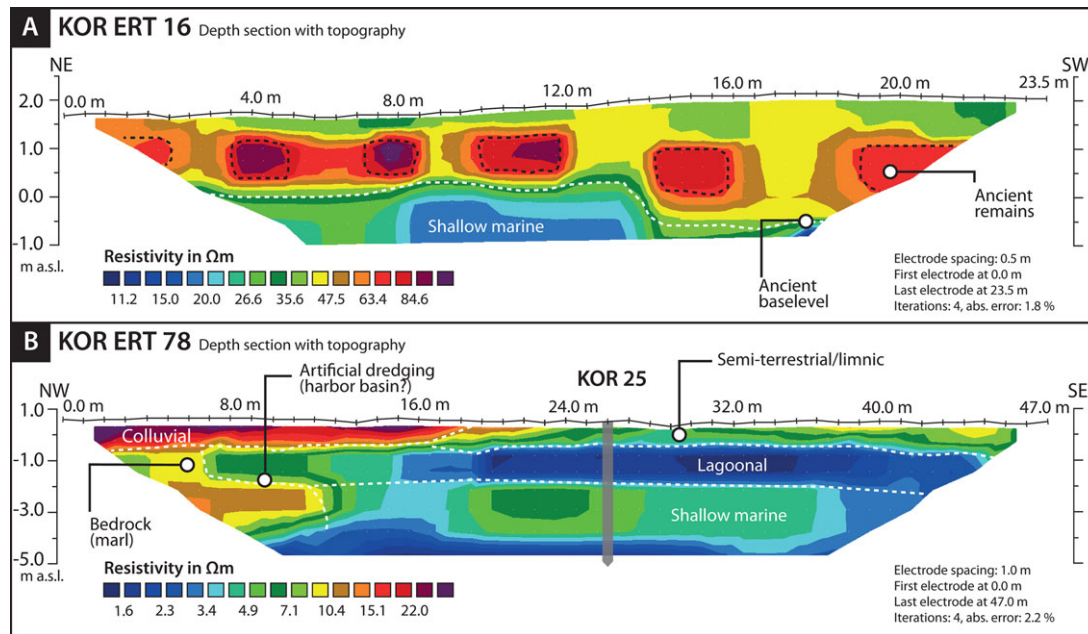


FIGURE 9 Results from electrical resistivity tomography measured along transects KOR ERT 16 (A) and KOR ERT 78 (B). For location of ERT transects see Figure 1

greater in lagoonal deposits, which also fits well with the low-energy depositional character of the lagoon-type environment.

In contrast to the lower lagoonal unit, the upper lagoonal sediments reveal markedly higher Pb concentrations. Pb was one of the first metals to be processed and therefore represents an excellent tracer for ancient human activities (Brännvall, Bindler, Emteryd, & Renberg, 2001; Véron, Goiran, Morhange, Marriner, & Empereur, 2006). As early as the 1st millennium B.C., Pb pollution appeared as a result of ore treatment and the byproduct of silver smelting (Hong, Candelone, Patterson, & Boutron, 1994; Lessler, 1988). During Roman times, Pb production reached extraordinarily high levels in places (Véron et al., 2006). Ancient Pb contamination has been documented in the Tiber River and Roman harbors of Portus, Marseille, and Sidon (Delile, Blichert-Toft, Goiran, Keay, & Albarède, 2014; Le Roux, Véron, & Morhange, 2003, 2005). Significantly increased Pb concentrations were also observed in ancient harbor deposits of Lechaion, Greece (Hadler et al., 2013); Kyllini, Greece (Hadler et al., 2015); and Tyre, Lebanon (Elmaleh et al., 2012). Thus, Pb and other trace metals can be powerful proxies for detecting ancient harbors (Marriner & Morhange, 2007). For the Alkinoos Harbor, natural sources of lead can be excluded, as the pre-lagoonal sediments are devoid of lead. Thus, we conclude that the upper lagoonal sediments encountered in cores KOR 1A, KOR 5, KOR 25, and KOR 24A are typical of ancient harbors (e.g., Hadler et al., 2013; Stock et al., 2013) and belong to the Alkinoos Harbor. Radiocarbon dates provide a *terminus post quem* of A.D. 78–128 and a *terminus ante quem* of A.D. 413–533 for these deposits (Table I). Thus, the detected harbor sediments document a harbor in use from the 1st to 6th century A.D. However, this age interval does not correspond to the age of the ancient shipsheds, which had originally been constructed in the early 5th century B.C. (Baika, 2013).

Vibracore KOR 2 was drilled in the proximity of a Roman installation (Baika, 2013) and offers a promising candidate for pre-Roman harbor sediments. The pre-Roman stratigraphic record of vibracore KOR 2 does not show silt-dominated harbor deposits but is dominated by sand. However, there is a section of silty sand encountered in the upper part of the core (Figure 4) that may indicate slightly reduced littoral dynamics of the shallow marine system. As the shipsheds were also founded upon shallow marine sand, this sedimentary unit most likely represents pre-Roman deposits associated with harbor installations.

Farther to the northwest, no pre-Roman harbor deposits were found in the stratigraphy of vibracore KOR 1A and cores of Transect II (Figure 1), where the Classical/Hellenistic harbor basin would have extended. Instead, thick Roman harbor mud overlies homogeneous shallow marine deposits, reflecting a stable open marine inner-shelf environment that had been established already in 6000 B.C. This stratigraphic gap and the presence of thick Roman harbor deposits are typical indicators for extensive Roman dredging (Marriner & Morhange, 2006). The Romans established a well-organized dredging technique, partly by using dredging ships, to prevent harbor basins closing from siltation and to preserve their navigability (Morhange & Marriner, 2010).

Dredging in the Alkinoos Harbor is also corroborated by geophysical findings from the western part of the study area. In transect KOR ERT 78 (Figure 9), a clearly delimited step-like structure within a unit of low resistivity, probably representing Miocene bedrock, is visible. This artificial structure, correlating well with the base of the lagoonal harbor mud, is suggested to represent a dredging contact with the bedrock. The eastern border of the dredged basin is represented by the walls encountered between vibracoring sites KOR 1A and KOR 2

because beyond the wall structures, at site KOR 2, the pre-Roman harbor record is still preserved (Figure 4).

Concerning the Roman harbor basin, our results enable a sedimentological and microfaunal differentiation between different parts of the harbor. Multiproxy data obtained for vibracore KOR 1A indicate a quiescent and sheltered basin. Only few, well-adapted microfaunal species were able to survive in this extreme and artificial environment. Due to subsequent siltation and desalinization, a low-energy quiescent environment evolved in this part of the harbor. In contrast, isochronous harbor sediments found at vibracoring site KOR 5 revealed a much higher energy level as documented by the presence of coarser-grained sediments and a different microfaunal association. Abundance and diversity of foraminifera are much higher, almost comparable with the foraminiferal fingerprint of the underlying shallow marine sand unit. Therefore, paleoenvironmental conditions within the harbor at vibracoring site KOR 5 must have been influenced by a steady inflow of salt-water and stable salinity conditions. Hence, we suggest that vibracoring site KOR 1A is located within a sheltered, perhaps isolated, inner part of the Roman Alkinoos Harbor, whereas vibracoring site KOR 5 was situated near a water inlet or entrance channel.

5.2 | The Alkinoos Harbor as sediment trap for paleotsunami impact

The stratigraphic record of vibracore KOR 1A drilled in front of the shipshed remains yielded typical harbor sediments, dated to Roman times. Our stratigraphic data further revealed two distinctly delimited sand layers. One sand layer intersects lagoonal muds, the other one was found overlying quiescent harbor deposits. Similar sand layers were also detected at vibracoring sites KOR 6A, KOR 25, and KOR 24A in the Alkinoos Harbor area. Torrential runoff from higher parts of the Analipsis Ridge can be excluded as the source of the sands because we found significant differences in grain-size and microfaunal content between the intersecting high-energy layers on the one hand, and the local marine bedrock, on the other hand (cf. Figures 4 and 5). Based on distinct sedimentological, geochemical, and micropaleontological features, we interpret these layers as the results of high-energy impact to the Alkinoos Harbor site associated with tsunami landfall.

Grain-size analyses revealed high amounts of medium to coarse sand and gravel indicating high-energy conditions (e.g., Goff & Chagué-Goff, 1999; Veerasingam et al., 2014; Vött et al., 2015; Yu, Zhao, Shi, & Meng, 2009), especially when compared to silt-dominated deposits of the quiescent and sheltered Roman harbor. Modern tsunami research has shown, for example, that onshore sand sheets are typical deposits associated with tsunami landfall (e.g., Shi, Dawson, & Smith, 1995). Moreover, the sand layers encountered in the Alkinoos Harbor basin show distinct peaks of the Ca/Fe ratio due to increasing input of calcium carbonate from the marine side in the form of shell debris and (micro)faunal tests (e.g., Goff & Chagué-Goff, 1999; Mathes-Schmidt et al., 2013; Sakuna, Szczuciński, Feldens, Schwarzer, & Khokiattiwong, 2012; Veerasingam et al., 2014; Vött et al., 2011b, 2015). The Alkinoos record also shows sedimentary features typical of high-energy impact such as erosional unconformities (KOR 1A, KOR 25, KOR 24A)

or fining upward sequences (KOR 24A; e.g., Bahlburg & Weiss, 2007; Gelfenbaum & Jaffe, 2003; Goff & Chagué-Goff, 1999; Morton, Gelfenbaum, & Jaffe, 2007; Shi et al., 1995).

Alkinoos Harbor sediments contained in vibracore KOR 1A are characterized by high Pb concentrations. In contrast, the high-energy sand layers show a strongly decreased Pb content, which we interpret as the result of a dilution effect by the input of marine waters and sediments, void of Pb (Hadler et al., 2013). Furthermore, even though coarser in grain-size, the intersecting sand layer in the harbor record of vibracore KOR 1A is characterized by higher electrical conductivity compared to fine-grained harbor sediments. This seems to be due to differences in the pore volume (influence of intruding salt water) as well as the content and composition of organic material.

Finally, the microfauna record of vibracore KOR 1A revealed striking differences between Alkinoos Harbor deposits and sand layers associated with abrupt shifts in faunal assemblages. As many species are able to adapt to gradually changing conditions (Sen Gupta, 1999; Murray, 2006), such abrupt shifts within foraminiferal assemblages point to sudden changes of crucial ecological parameters. In the case of the Alkinoos Harbor, abrupt changes were obviously associated with the temporary and high-energy input of marine water and sediments into the harbor basin so that the preexisting harbor ecosystem was profoundly disturbed (e.g., Goff et al., 2000; Hawkes et al., 2007; Shennan et al., 1996). A further characteristic of a high-energy event are strongly mixed foraminiferal assemblages (e.g., Briggs et al., 2014; Dominey-Howes, Humphreys, & Hesse, 2006; Mamo et al., 2009; Pilarczyk et al., 2014) as tsunami waters may erode, transport, and rework allochthonous sediments from the different shelf and littoral zones (Goff, Chagué-Goff, & Nichol, 2001). Within the sand layers of vibracore KOR 1A, we found species preferring littoral environments and species typical of harbor conditions. In addition, new, exotic species were found that are predominantly adapted to cold and deep water from areas farther away from the inner shelf (Murray, 2006). Such species were not found in the autochthonous shallow marine sands below. Mamo et al. (2009) consider this as a key diagnostic characteristic for tsunami-deposited sediments.

These multiproxy features clearly indicate that the ecological harbor system was repeatedly interrupted by short-term high-energy impacts from the sea. In general and on a global scale, the differentiation between high-energy storm and tsunami influence based on diagnostic sedimentary data is highly problematic, because some high-energy features may be caused by both storm and tsunami impact (e.g., Morton et al., 2007; Switzer & Jones, 2008). For this reason, the natural wave climate of the wider study area has to be taken into consideration. The open Ionian Sea shows mean significant wave heights of 1.2–1.6 m (Cavaleri, 2005)—its northern part and the neighboring Adriatic Sea are known for the lowest significant wave heights in the whole Mediterranean (Lionello et al., 2012). Wave data recorded near the Ionian island of Zakynthos, lying some 200 km to the southeast of Corfu, show a mean significant wave height of less than 1 m (HCMR, 2015) attesting to a very low annual wave energy level (Karathanasi, Soukissian, & Sifnioti, 2015). However, heavy storms may occur frequently, often linked to Sirocco or tropical-type cyclones (Llasat, 2009), which are a known phenomenon during

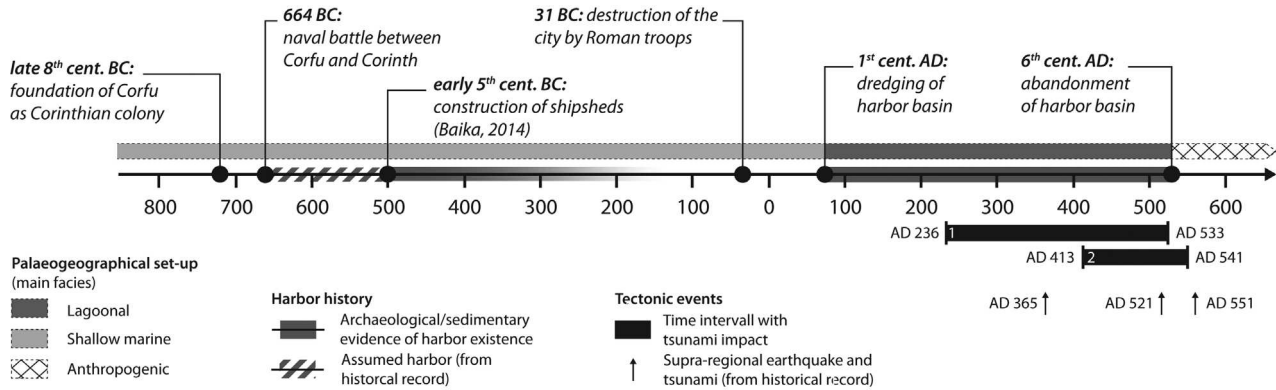


FIGURE 10 Schematic timeline with the main historical events concerning ancient Corfu and major geoaarchaeological findings from this study. The pre-Roman Alkinoos Harbor naval installations were built on a sandy seashore. The Roman Alkinoos Harbor, a sheltered and quiescent basin, was used between the late 1st and early 6th century A.D. It experienced two high-energy events related to tsunami landfall between the late 3rd and the early 6th century and between the beginning of the 5th and mid-6th century A.D., most probably associated with the supraregional A.D. 365 and A.D. 521/551 events, respectively

winter and autumn. The track lines of such “medicanes” usually run farther south, but they may occur in the Ionian Sea as well (e.g., Campins, Genovés, Picornell, & Jansà, 2011; Davolio et al., 2009). Ghionis et al. (2015) found evidence of significant wave heights of more than 5 m offshore Lefkada Island, while maximum observed wave heights of 7 m are reported for the coasts of Sicily (Scicchitano, Monaco, & Tortorici, 2007). Nevertheless, as already stated, ancient Corfu is located at the shore of the narrow Gulf of Corfu. This gulf is located between Corfu Island and the Greek-Albanian mainland. It is up to 70 m deep and at most 30 km wide. The northern entrance to the gulf is only 2 km wide, while its southern entrance measures 8 km in width. Due to its sheltered position, the influence of wind-generated waves from the northwest is thus reduced to a minimum. Waves within the lake-like Gulf of Corfu reach less than 1 m in height (Lionello et al., 2012; Mazarakis, Kotroni, Lagouvardos, & Bertotti, 2012). Thus, the Gulf of Corfu is one of the best protected natural harbors of the entire Mediterranean.

Based on local geography and wave climate data, storms can be excluded *a priori* as a cause for the high-energy sediments detected in the Alkinoos Harbor geoarchive, as storm-generated waves in the Gulf of Corfu are not able to deposit thick and widespread high-energy sand sheets as encountered in the Alkinoos Harbor area. Instead, tsunamis as high magnitude and low-frequency events must be considered, especially when taking into account Corfu’s location within this seismically active region in the Mediterranean. Several geoscientific studies have revealed that the island of Corfu was subject to repeated local co-seismic movements (Evelpidou et al., 2014; Mastronuzzi et al., 2014; Pirazzoli et al., 1994). Such crustal movements may have been associated with local tsunami phenomena. Apart from such local seismic origins, tsunamis may also hit Corfu in the form of teletsunamis originating along the Hellenic Trench as major seismic zone in the Mediterranean. The high tsunami hazard of Corfu is also reflected by the large number of entries found in earthquake and tsunami catalogues for the northern Ionian Sea around Corfu Island (Hadler et al., 2012; Stiros, Pirazzoli, Laborel, & Laborel-Deguen, 1994). Finally, Fischer et al. (2016a), for the first time, report on geomorphological and

sedimentary traces of repeated tsunami impact in two lagoonal environments on Corfu.

Our findings document two discrete tsunami inundation phases for the Alkinoos Harbor (Figure 10). The harbor unit immediately underneath the first tsunami layer is radiocarbon dated to A.D. 78–128 (KOR 1A/24+ HR). This date is considered as *terminus ad* or *post quem* for the event. In addition, the sediments overlying the tsunami deposit yielded a *terminus ante quem* of A.D. 413–533 (KOR 1A/9+ HK). The first tsunami must therefore have occurred between the late 1st and the early 6th century A.D. Another sample was taken from the tsunami layer itself and dated to A.D. 236–325 (KOR 1A/21+ PR). Due to possible reworking effects, this age has to be considered a maximum age for the event. We finally conclude that the first event took place between the late 3rd and the early 6th century A.D. It is highly probable that it is related to the well-known earthquake and tsunami that hit the Mediterranean world on July 21st A.D. 365.

The A.D. 365 earthquake had its origin on Crete, but its effects were felt as far as the northern edge of the Ionian Sea (Shaw, 2012; Shaw et al., 2008). Our geoaarchaeological data from the Alkinoos Harbor strongly support the idea that the A.D. 365 event hit the Gulf of Corfu as teletsunami entering the bottleneck-type gulf from the south. This conclusion is also supported by numerical simulation results recently published by Fischer et al. (2016a) that define the hydrodynamic constellations and potential geomorphodynamic consequences associated with a hypothetical near-coast tsunami wave, 2.5 m high, approaching Corfu from different directions. In these scenarios, modeling results revealed strongest tsunami inundation of the inner Gulf of Corfu by tsunami waves approaching from the south (Fischer et al., 2016a). This hydrodynamic pattern has also to be assumed for the A.D. 365 tsunami event. Based on numerical models, Shaw et al. (2008) showed that teletsunami effects of the A.D. 365 tsunami impact generally hit Corfu from a southern direction. The height of the A.D. 365 tsunami waves at the southern entrance to the Gulf of Corfu is certainly controlled by shoaling effects bound to the shelf topography and to hydrodynamic local-scale effects bound to funneling, refraction, and diffraction of tsunami waters. Based on these general flow patterns (Fischer et al.

2016a; Shaw et al. 2008), we therefore hypothesize that the Gulf of Corfu was directly affected by the A.D. 365 tsunami event. This is also supported by sedimentary evidence that was found along the coasts of Sicily (De Martini et al., 2012; Smedile et al., 2011) and adjacent coasts of northwestern Greece (May et al., 2012; Vött et al., 2009) proving that the A.D. 365 tsunami reached the northernmost parts of the Ionian Sea. The scenario of an A.D. 365 tsunami landfall on Corfu is thus more than likely.

Based on our results, a second tsunami event occurred between A.D. 413–533 (KOR 1A/9+ HK; *terminus ad or post quem*) and A.D. 430–541 (KOR 1A/6+ HK; *terminus ante quem*; Figure 3), namely between the beginning 5th and mid-6th century A.D. Traces of this event were found in vibracore KOR 5, where the upper harbor sediments show increased input of fine sand. In a supraregional context, radiocarbon dates for this event correlate well with historical records of a series of severe earthquakes and associated tsunamis that occurred in A.D. 521 and A.D. 551 as registered by modern seismological catalogues for the Gulf of Corinth (Ambraseys & Synolakis, 2010; Hadler et al., 2012; Soloviev et al., 2000). This relation, however, remains speculative as the spatial extent of these historic events beyond the Gulf of Corinth is in question and not proven by historical accounts. However, traces of tsunami impact in the 6th century A.D. are also known from across the eastern Mediterranean, for instance from the Levantine coast (Goodman-Tchernov, Dey, Reinhardt, McCoy, & Mart, 2009) and the western Peloponnese (Vött et al., 2011a). Beyond this question, the second historical event detected in the Alkinoos Harbor geoarchive provides a *terminus post quem* for the abandonment of the harbor, as these event deposits, lying on top of harbor sediments, are buried underneath anthropogenic infill.

6 | CONCLUSIONS

The focus of our geoarchaeological study was to detect and investigate the geoarchive of the ancient Alkinoos Harbor thus far ascertained by archaeological excavation of harbor facilities, mainly shipshed remains. Our main objectives were to reconstruct coastline shifts and paleoenvironmental changes and infer related human-environmental interactions. Methodologically, we carried out detailed sedimentological, geophysical, microfaunal, and geochemical investigations using a multi-proxy approach. The main conclusions can be summarized as follows:

- (i) For the first time, sedimentary evidence of a harbor situation was found and analyzed. Harbor deposits were identified by their characteristic silt-dominant grain-size, by their richness in organic material, and, finally, by distinctly high amounts of Pb as a tracer for human activity. Sediments encountered suggest a closed and protected, low-energy harbor environment, at least for the Roman period.
- (ii) Based on geochronological data, the harbor was in use between the late 1st and early 6th century A.D. The pre-Roman harbor basin, associated with the shipshed complex of the early 5th century B.C., was not clearly traced in the sedimentary record. As a result, we assume that at least a considerable part of the Classical/Hellenistic harbor sediments was removed by extensive Roman dredging in the 1st century A.D. The dredged Roman harbor basin was traced over a distance of 160 m in an east–west direction (KOR 1A, KOR 5, KOR 24A). Its eastern border seems to be represented by a wall structure situated between vibracores KOR 1A and KOR 2.
- (iii) Grain-size data and microfaunal assemblages reveal a significant difference between the eastern and western parts of the Roman harbor. Whereas the eastern part (KOR 1A, Figures 4 and 5) is characterized by fine-grained sediments deposited in a quiescent low-energy zone, the western part (KOR 5, Figures 7 and 8) seemed to be partly exposed to higher dynamics and sea water influence. We suppose that there was a harbor entrance or channel close to site KOR 5.
- (iv) Pre-Roman harbor deposits were found in vibracore KOR 2 (Figure 4) drilled close to a Roman installation. These older harbor deposits are dominated by silty sand of a beach facies. This fits well with geophysical and stratigraphic data as well as archaeological stratigraphy, documenting that the Alkinoos shipsheds were founded on fine sand.
- (v) We found two distinct high-energy sand layers intersecting Roman Alkinoos Harbor mud, which we interpret as evidence of periodic tsunami landfall on Corfu Island (Figure 10). Tsunami deposits are characterized by erosional contacts, fining upward of grain-size, and a distinctly allochthonous microfaunal fingerprint. Based on radiocarbon dating, the first event occurred between the late 3rd and the early 6th century A.D. and most probably corresponds to the A.D. 365 earthquake (Crete) and tsunami event. The second event took place between the beginning 5th and mid-6th century A.D. By interpretation of our geomorphological and geochronological evidence, both tsunami layers are thus considered to be the results of teletsunami impact and not generated by local fault movements. The Alkinoos Harbor has proved to be an excellent sediment trap for paleotsunami signatures.

ACKNOWLEDGMENTS

This paper presents the results of an interdisciplinary project directed by the Ephorate of Antiquities of Corfu, in collaboration with the Institute of Geography at the Johannes Gutenberg-Universität Mainz, Germany, associated with the Centre Camille Jullian, CNRS at the Aix-Marseille Université, France. We are kindly indebted to the personnel of the Ephorate of Antiquities of Corfu, mainly topographer Stefanos Armenis, archaeologists Alexis Paramythiotis, Alexis Alexis, Alexia Tralou, and Elena Bonelou, architects Kleio Krasaki and Nausika Mandila for their precious help and various support during the field campaigns. We would also like to thank G. Mastronuzzi (Bari) and an anonymous reviewer for careful reading and valuable comments that helped to improve the manuscript.

REFERENCES

Ad Hoc-Arbeitsgruppe Boden. (2005). *Bodenkundliche Kartieranleitung*. Stuttgart: E. Schweizerbart'sche Verlagsbuchhandlung.

- Albini, P. (2004). A survey of the past earthquakes in the Eastern Adriatic (14th to early 19th century). *Annals of Geophysics*, 47, 675–703.
- Algan, O., Yalçın, M. N., Özdoğan, M., Yılmaz, İ., Sarı, E., Kırıcı-Elmas, E., ... Karamut, İ. (2009). A short note on the geo-archeological significance of the ancient Theodosius harbor (İstanbul, Turkey). *Quaternary Research*, 72, 457–461.
- Algan, O., Yalçın, M. N., Özdoğan, M., Yılmaz, Y., Sarı, E., Kırıcı-Elmas, E., ... Meriç, E. (2011). Holocene coastal change in the ancient harbor of Yenikapı–İstanbul and its impact on cultural history. *Quaternary Research*, 76, 30–45.
- Ambraseys, N., & Synolakis, C. (2010). Tsunami catalogs for the Eastern Mediterranean, revisited. *Journal of Earthquake Engineering*, 14, 309–330.
- Babbucci, D., Tamburelli, C., Viti, M., Mantovani, E., Albarello, D., D'Onza, F., ... Mugnaioli, E. (2004). Relative motion of the Adriatic with respect to the confining plates: Seismological and geodetic constraints. *Geophysical Journal International*, 159, 765–775.
- Bahlburg, H., & Weiss, R. (2007). Sedimentology of the December 26, 2004, Sumatra tsunami deposits in eastern India (Tamil Nadu) and Kenya. *International Journal of Earth Sciences*, 96, 1195–1209.
- Baika, K. (2003). ΝΕΩΣΟΙΚΟΙ. *Installations navales en Méditerranée. Les neoria de Corcyre* (Unpublished doctoral thesis). Université de Paris I (Panthéon-Sorbonne), Paris.
- Baika, K. (2013). Corcyra (Corfu). In D. Blackman, B. Rankov, K. Baika, H. Gerding, & J. Pakkanen (Eds.), *Shipsheds of the ancient Mediterranean* (pp. 319–334). Cambridge: Cambridge University Press.
- Baika, K. (2015). Ancient harbor cities—New methodological perspectives and recent research in Greece. In S. Ladstätter, F. Pirson, & T. Schmidts (Eds.), *Harbors and harbor cities in the Eastern Mediterranean from Antiquity to the Byzantine period. Recent Discoveries & New Approaches, Proceedings of the International Symposium (DAI), BYZAS 19* (= Österreichisches Archäologisches Institut Sonderband 52) (Vol. II, pp. 445–491). Istanbul: Ege Yayınları.
- Barbano, M. S., Pirrotta, C., & Gerardi, F. (2010). Large boulders along the south-eastern Ionian coast of Sicily: Storm or tsunami deposits? *Marine Geology*, 275, 140–154.
- Battaglia, M., Murray, M. H., Serpelloni, E., & Bürgmann, R. (2004). The Adriatic region: An independent microplate within the Africa-Eurasia collision zone. *Geophysical Research Letters*, 31(9), L09605.
- Bini, M., Chelli, A., Durante, A. M., Gervasini, L., & Pappalardo, M. (2009). Geoarchaeological sea-level proxies from a silted up harbour: A case study of the Roman colony of Luni (northern Tyrrhenian Sea, Italy). *Quaternary International*, 206, 147–157.
- Blackman, D., Rankov, B., Baika, K., Gerding, H., & Pakkanen J. (Eds.). (2013). *Shipsheds of the Ancient Mediterranean* (pp. 319–334). Cambridge: Cambridge University Press.
- Blackman, D. J. (1982). Ancient harbours in the Mediterranean. Part 2. *International Journal of Nautical Archaeology and Underwater Exploration*, 11, 185–211.
- Blume, H.-P., Stahr, K., & Leinweber, P. (2011). *Bodenkundliches Praktikum*. Heidelberg: Spektrum.
- Bony, G., Marriner, N., Morhange, C., Kaniewski, D., & Perinçek, D. (2012). A high-energy deposit in the Byzantine harbour of Yenikapı, Istanbul (Turkey). *Quaternary International*, 266, 117–130.
- Brännvall, M.-L., Bindler, R., Emteryd, O., & Renberg, I. (2001). Four thousand years of atmospheric lead pollution in northern Europe: A summary from Swedish lake sediments. *Journal of Paleolimnology*, 25, 421–435.
- Briggs, R. W., Engelhart, S. E., Nelson, A. R., Dura, T., Kemp, A. C., Haeussler, P. J., ... Bradley, L.-A. (2014). Uplift and subsidence reveal a nonpersistent megathrust rupture boundary (Sitkinak Island, Alaska). *Geophysical Research Letters*, 41(7), 2289–2296.
- Campins, J., Genovés, A., Picornell, M. A., & Jansà, A. (2011). Climatology of Mediterranean cyclones using the ERA-40 dataset. *International Journal of Climatology*, 31, 1596–1614.
- Cavaleri, L. (2005). The wind and wave atlas of the Mediterranean Sea—The calibration phase. *Advances in Geoscience*, 2, 255–257.
- Cimerman, F., & Langer, M. R. (1991). Mediterranean formaminifera. Ljubljana: Slovenska Akademija Znanosti in Umetnosti.
- Davolio, S., Miglietta, M. M., Moscatello, A., Pacifico, F., Buzzi, A., & Rotunno, R. (2009). Numerical forecast and analysis of a tropical-like cyclone in the Ionian Sea. *Natural Hazards and Earth System Science*, 9, 551–562.
- De Martini, P. M., Barbano, M. S., Pantosti, D., Smedile, A., Pirrotta, C., Del Carlo, P., & Pinzi, S. (2012). Geological evidence for paleotsunamis along eastern Sicily (Italy): An overview. *Natural Hazards and Earth System Science*, 12, 2569–2580.
- Delile, H., Abichou, A., Gadhoum, A., Goiran, J.-P., Pleuger, E., Monchambert, J.-Y., ... Ghazzi, F. (2015). The geoarchaeology of Utica, Tunisia: The paleogeography of the Mejerda Delta and hypotheses concerning the location of the Ancient Harbor. *Geoarchaeology*, 30, 291–306.
- Delile, H., Blichert-Toft, J., Goiran, J.-P., Keay, S., & Albarède, F. (2014). Lead in ancient Rome's city waters. *Proceedings of the National Academy of Sciences*, 111, 6594–6599.
- Di Bella, L., Bellotti, P., Frezza, V., Bergamin, L., & Carboni, M. G. (2011). Benthic foraminiferal assemblages of the imperial harbor of Claudius (Rome): Further paleoenvironmental and geoarchaeological evidences. *Holocene*, 21, 1245–1259.
- Dominey-Howes, D., Cundy, A., & Croudace, I. (2000). High energy marine flood deposits on Astypalaea Island, Greece: Possible evidence for the A.D. 1956 southern Aegean tsunami. *Marine Geology*, 163, 303–315.
- Dominey-Howes, D. T. M., Humphreys, G. S., & Hesse, P. P. (2006). Tsunami and palaeotsunami depositional signatures and their potential values in understanding the late-Holocene tsunami record. *Holocene*, 16, 1095–1107.
- Dontas, G. (1965). Τοπογραφικά θέματα της πολιορκίας της Κέρκυρας του έτους 373 π.Χ. (Topographical issues of the siege of Corcyra in 373 B.C.). *Archaiologiki Ephimeris*, 1965, 139–144.
- Dontas, G. (1966). Ανασκαφαί Κέρκυρας (Excavations at Corcyra). *Praktika Archaeologikis Etaireias*, 1966, 85–94.
- Elmaleh, A., Galy, A., Allard, T., Dairon, R., Day, J. A., Michel, F., ... Couffignal, F. (2012). Anthropogenic accumulation of metals and metalloids in carbonate-rich sediments: Insights from the ancient harbor setting of Tyre (Lebanon). *Geochimica et Cosmochimica Acta*, 82, 23–38.
- Evelpidou, N., Karkani, A., & Pirazzoli, P. A. (2014). Fossil shorelines at Corfu and surrounding islands deduced from erosional notches. *Holocene*, 24, 1565–1572.
- Faivre, S., Fouache, E., Ghilardi, M., Antonoli, F., Furlani, S., & Kovačić, V. (2011). Relative sea level change in western Istria (Croatia) during the last millennium. *Quaternary International*, 232, 132–143.
- Fischer, P., Finkler, C., Rübke, B. R., Baika, K., Hadler, H., Willershäuser, T., ... Vött, A. (2016a). Impact of Holocene tsunamis detected in lagoonal environments on Corfu (Ionian Islands, Greece)—Geomorphological, sedimentary and microfaunal evidence. *Quaternary International*, 401, 4–16.
- Fischer, P., Wunderlich, T., Rabbel, W., Vött, A., Willershäuser, T., Baika, K., ... Metallinou, G. (2016b). Combined electrical resistivity tomography (ERT), direct-push electrical conductivity logging (DP-EC) and vibracoring—A new methodological approach in geoarchaeological research. *Archaeological Prospection*, 23(3), 213–228.

- Fouache, E., Dalongeville, R., Kunesch, S., Suc, J.-P., Subally, D., Prieur, A., & Lozouet, P. (2005). The environmental setting of the harbor of the classical site of Oeniades on the Acheloos Delta, Greece. *Geoarchaeology*, 20, 285–302.
- Gehrke, H.-J., & Wirbelauer, E. (2004). Korkyra. In M. H. Hansen & T. H. Nielsen (Eds.), *An inventory of archaic and classical poleis* (pp. 361–363). Oxford: Oxford University Press.
- Gelfenbaum, G., & Jaffe, B. (2003). Erosion and sedimentation from the 17 July, 1998 Papua New Guinea tsunami. *Pure and Applied Geophysics*, 160, 1969–1999.
- Ghionis, G., Poulos, S. E., Verykiou, E., Karditsa, A., Alexandrakis, G., & Andris, P. (2015). The impact of an extreme storm event on the Barrier Beach of the Lefkada Lagoon, NE Ionian Sea (Greece). *Mediterranean Marine Science*, 16(3), 562–572.
- Goff, J. R., & Chagué-Goff, C. (1999). A late Holocene record of environmental changes from coastal wetlands: Abel Tasman National Park, New Zealand. *Quaternary International*, 56, 39–51.
- Goff, J., Chagué-Goff, C., & Nichol, S. (2001). Palaeotsunami deposits: A New Zealand perspective. *Sedimentary Geology*, 143, 1–6.
- Goff, J. R., Rouse, H. L., Jones, S. L., Hayward, B. W., Cochran, U., McLea, W., ... Morley, M. S. (2000). Evidence for an earthquake and tsunami about 3100±3400 yr ago, and other catastrophic saltwater inundations recorded in a coastal lagoon, New Zealand. *Marine Geology*, 170, 213–249.
- Goiran, J.-P., Salomon, F., Mazzini, I., Bravard, J.-P., Pleuger, E., Vittori, C., ... Sadori, L. (2014). Geoarchaeology confirms location of the ancient harbour basin of Ostia (Italy). *Journal of Archaeological Science*, 41, 389–398.
- Goodman, B. N., Reinhardt, E. G., Dey, H. W., Boyce, J. I., Schwarcz, H. P., Sahoğlu, V., ... Artzy, M. (2009). Multi-proxy geoarchaeological study redefines understanding of the paleocoastlines and ancient harbours of Liman Tepe (Iskele, Turkey). *Terra Nova*, 21, 97–104.
- Goodman-Tchernov, B. N., Dey, H. W., Reinhardt, E. G., McCoy, F., & Mart, Y. (2009). Tsunami waves generated by the Santorini eruption reached Eastern Mediterranean shores. *Geology*, 37, 943–946.
- Hadler, H., Baika, K., Pakkanen, J., Evangelistis, D., Emde, K., Fischer, P., ... Vött, A. (2015). Palaeotsunami impact on the ancient harbour site Kyllini (western Peloponnese, Greece) based on a geomorphological multi-proxy approach. *Zeitschrift für Geomorphologie N.F., Supplementary Issue*, 59(4), 7–41.
- Hadler, H., Vött, A., Brückner, H., Bareth, G., Ntageretzi, K., Warnecke, H., & Willershäuser, T. (2011). The harbor of ancient Krane, Kutavos Bay (Cefalonia, Greece)—An excellent geo-archive for palaeo-tsunami research. In V. Karius, H. Hadler, M. Deicke, H. Van Eynatter, H. Brückner, & A. Vött (Eds.), *Dynamische Küsten—Grundlagen, Zusammenhänge und Auswirkungen im Spiegel angewandter Küstenforschung*. Coastline Reports 17 (pp. 111–122). Rostock: EUCC.
- Hadler, H., Vött, A., Koster, B., Mathes-Schmidt, M., Mattern, T., Ntageretzi, K., ... Willershäuser, T. (2013). Multiple late-Holocene tsunami landfall in the eastern Gulf of Corinth recorded in the palaeotsunami geo-archive at Lechaion, harbour of ancient Corinth (Peloponnese, Greece). *Zeitschrift für Geomorphologie N.F., Supplementary Issue*, 57(4), 139–180.
- Hadler, H., Willershäuser, T., Ntageretzi, K., Henning, P., & Vött, A. (2012). Catalogue entries and non-entries of earthquake and tsunami events in the Ionian Sea and the Gulf of Corinth (eastern Mediterranean, Greece) and their interpretation with regard to palaeotsunami research. In A. Vött & J.-F. Venzke (Eds.), *Beiträge der 29. Jahrestagung des Arbeitskreises „Geographie der Meere und Küsten“*, 28. bis 30. April 2011 in Bremen. Bremer Beiträge zur Geographie und Raumplanung, 44, 1–15.
- Harrington, G. A., & Hendry, M. J. (2006). Using Direct-Push EC logging to delineate heterogeneity in a clay-rich aquitard. *Ground Water Monitoring & Remediation*, 26(1), 92–100.
- Hawkes, A. D., Bird, M., Cowie, S., Grundy-Warr, C., Horton, B. P., Hwai, A. T. S., ... Aik, L. W. (2007). Sediments deposited by the 2004 Indian Ocean Tsunami along the Malaysia–Thailand Peninsula. *Marine Geology*, 242, 169–190.
- HCMR—Hellenic Center for Marine Research. (2015). Poseidon Data Base Web: <http://www.poseidon.hcmr.gr/listview.php?id=136> (last access on 07-30-2016).
- Hollenstein, C., Müller, M., Geiger, A., & Kahle, H. G. (2008). Crustal motion and deformation in Greece from a decade of GPS measurements, 1993–2003. *Tectonophysics*, 449, 17–40.
- Hong, S., Candelone, J.-P., Patterson, C. C., & Boutron, C. F. (1994). Greenland ice evidence of hemispheric lead pollution two millennia ago by Greek and Roman civilizations. *Science*, 265, 1841–1843.
- IGME—Institute of Geology and Mineral Exploration (Ed.). (1970). Geological Map of Greece—Sheet North and South Corfu. Scale 1:50,000. Athens.
- Kanta-Kitsou, A. (2001). Ένας νεώσοικος, τμήμα των νεορίων του Υλλαϊκού λιμανιού της Αρχαίας Κέρκυρας (A shipshed, section of the neorion of the Hyliaikos Harbour of ancient Corcyra). In H. Tzalas (Ed.), *Tropis VI. 6th International Symposium on Ship Construction in Antiquity, Lamia 1996* (pp. 273–299). Athens: Hellenic Institute for the Preservation of Nautical Tradition.
- Karathanasi, F., Soukissian, T., & Sifnioti, D. (2015). Offshore wave potential of the Mediterranean Sea. *Renewable Energy and Power Quality Journal*, 13, 461–465.
- Keary, P., Brooks, M., & Hill, I. (2002). An introduction to geophysical exploration. Malden, Oxford, and Carlton: Blackwell Science.
- Kiechle, F. K. (1979). Korkyra und der Handelsweg durch das Adriatische Meer im 5. Jh. v. Chr. *Historia: Zeitschrift für Alte Geschichte*, 28, 173–191.
- Kokkalas, S., Xypolias, P., Koukouvelas, I., & Doutsos, T. (2006). Postcollisional contractional and extensional deformation in the Aegean region. In Y. Dilek & S. Pavlides (Eds.), *Postcollisional tectonics and magmatism in the Mediterranean region and Asia* (pp. 97–127). Boulder: The Geological Society of America.
- Kraft, J. C., Rapp, G., Kayan, I., & Luce, J. V. (2003). Harbor areas at ancient Troy: Sedimentology and geomorphology complement Homer's Iliad. *Geology*, 31, 163–166.
- Le Roux, G., Véron, A., & Morhange, C. (2003). Geochemical evidences of early anthropogenic activity in harbour sediments from Sidon. *Archaeology and History in Lebanon*, 18, 115–118.
- Le Roux, G., Véron, A., & Morhange, C. (2005). Lead pollution in the ancient harbours of Marseille. *Méditerranée*, 1, 31–35.
- Lehmann-Hartleben, K. (1923). Die antiken Hafenanlagen des Mittelmeeres. *Beiträge zur Geschichte des Städtebaus im Altertum. Klio: Beiträge zur alten Geschichte, Beiheft XIV*. Leipzig: Dietrich'sche Verlagsbuchhandlung.
- Lessler, M. A. (1988). Lead and lead poisoning from antiquity to modern times. *Ohio Journal of Science*, 88(3), 78–84.
- Lionello, P., Abrantes, F., Congedi, L., Dulac, M. G., Gomis, D., Goodess, C., ... Xoplaki, E. (2012). Introduction: Mediterranean climate—background information. In P. Lionello (Ed.), *The climate of the Mediterranean region. From the past to the future* (pp. xxxv–xc). London: Elsevier.
- Llasat, M. C. (2009). High magnitude storms and floods. In J. C. Woodward (Ed.), *The physical geography of the Mediterranean* (pp. 513–540). Oxford: University Press.
- Loeblich, A. R., & Tappan, H. N. (1988). Foraminiferal genera and their classification. New York: Springer.
- Loke, M. H., Acworth, I., & Dahlin, T. (2003). A comparison of smooth and blocky inversion methods in 2D electrical imaging surveys. *Exploration Geophysics*, 34, 182–187.

- Loke, M. H., & Dahlin, T. (2002). A comparison of the Gauss–Newton and quasi-Newton methods in resistivity imaging inversion. *Journal of Applied Geophysics*, 49, 149–162.
- Mamo, B., Strotz, L., & Dominey-Howes, D. (2009). Tsunami sediments and their foraminiferal assemblages. *Earth-Science Reviews*, 96, 263–278.
- Maramai, A., Graziani, L., & Tinti, S. (2007). Investigation on tsunami effects in the central Adriatic Sea during the last century—A contribution. *Natural Hazards and Earth System Science*, 7, 15–19.
- Marriner, N., & Morhange, C. (2006). Geoarchaeological evidence for dredging in Tyre's ancient harbour, Levant. *Quaternary Research*, 65, 164–171.
- Marriner, N., & Morhange, C. (2007). Geoscience of ancient Mediterranean harbours. *Earth-Science Reviews*, 80, 137–194.
- Marriner, N., Morhange, C., Faivre, S., Flaux, C., Vacchi, M., Miko, S., ... Radic Rossi, I. (2014). Post-Roman sea-level changes on Pag Island (Adriatic Sea): Dating Croatia's "enigmatic" coastal notch? *Geomorphology*, 221, 83–94.
- Mastronuzzi, G., Calcagnile, L., Pignatelli, C., Quarta, G., Stamatopoulos, L., & Venisti, N. (2014). Late Holocene tsunamigenic uplift in Kerkira Island, Greece. *Quaternary International*, 332, 48–60.
- Mastronuzzi, G., Pignatelli, C., Sansó, P., & Selli, G. (2007). Boulder accumulations produced by the 20th February 1743 tsunami along the coast of southeastern Salento. *Marine Geology*, 242, 191–205.
- Mastronuzzi, G., & Sansó, P. (2004). Large boulder accumulations by extreme waves along the Adriatic coast of southern Apulia (Italy). *Quaternary International*, 120, 173–184.
- Mathes-Schmidt, M., Schwarzbauer, J., Papanikolaou, I., Syberberg, F., Thiele, A., Wittkopp, F., & Reicherter, K. (2013). Geochemical and micropaleontological investigations of tsunamigenic layers along the Thracian Coast (Northern Aegean Sea, Greece). *Zeitschrift für Geomorphologie N.F., Supplementary Issue*, 57(4), 5–27.
- May, S. M., Vött, A., Brückner, H., Grapmayer, R., Handl, M., & Wennrich, V. (2012). The Lefkada barrier and beachrock system (NW Greece)—Controls on coastal evolution and the significance of extreme wave events. *Geomorphology*, 139–140, 330–347.
- Mazarakis, N., Kotroni, V., Lagouvardos, K., & Bertotti, L. (2012). High-resolution wave model validation over the Greek maritime areas. *Natural Hazards and Earth System Science*, 12, 3433–3440.
- Mazzini, I., Faranda, C., Giardini, M., Giraudi, C., & Sadori, L. (2011). Late Holocene palaeoenvironmental evolution of the Roman harbour of Portus, Italy. *Journal of Paleolimnology*, 46, 243–256.
- Millet, B., Tronchère, H., & Goiran, J.-P. (2014). Hydrodynamic modeling of the Roman Harbor of Portus in the Tiber Delta: The impact of the north-eastern channel on current and sediment dynamics. *Geoarchaeology*, 29, 357–370.
- Morhange, C., Blanc, F., Schmitt-Mercury, S., Bourcier, M., Carbonel, P., Oberlin, C., ... Hesnard, A. (2003). Stratigraphy of late-Holocene deposits of the ancient harbour of Marseilles, southern France. *Holocene*, 14(4), 593–604.
- Morhange, C., & Marriner, N. (2010). Mind the (stratigraphic) gap: Roman dredging in ancient Mediterranean harbours. *Bollettino di Archeologia*, on line, B/B7/4, 23–32.
- Morhange, C., Marriner, N., & Carayon, N. (2014). The geoarchaeology of ancient Mediterranean harbours. In N. Carcaud & G. Arnaud-Fassetta (Eds.), *La géoarchéologie française au XXI^e siècle* (pp. 245–254). Paris: CNRS Edition.
- Morton, R. A., Gelfenbaum, G., & Jaffe, B. E. (2007). Physical criteria for distinguishing sandy tsunami and storm deposits using modern examples. *Sedimentary Geology*, 200, 184–207.
- Mourtzas, N. D., Kissas, C., & Kolaiti, E. (2014). Archaeological and geomorphological indicators of the historical sea level changes and the related palaeogeographical reconstruction of the ancient foreharbour of Lechaion, East Corinth Gulf (Greece). *Quaternary International*, 332, 151–171.
- Murray, J. W. (2006). *Ecology and applications of benthic foraminifera*. Cambridge: Cambridge University Press.
- Partsch, J. (1887). Die Insel Korfu. Eine geographische Monographie. *Petermanns Mitteilungen, Ergänzungsheft* 88. Gotha: Justus Perthes.
- Pilarczyk, J. E., Dura, T., Horton, B. P., Engelhart, S. E., Kemp, A. C., & Sawai, Y. (2014). Microfossils from coastal environments as indicators of paleo-earthquakes, tsunamis and storms. *Palaeogeography, Palaeoclimatology, Palaeoecology*, 413, 144–157.
- Pirazzoli, P. A., Stiros, S. C., Laborel, J., Laborel-Deguen, F., Arnold, M., Papa-georgiou, S., & Morhange, C. (1994). Late-Holocene shoreline changes related to palaeoseismic events in the Ionian Islands, Greece. *Holocene*, 4, 397–405.
- Poulos, S. E., Lykousis, V., Collins, M. B., Rohling, E. J., & Pattiaratchi, C. B. (1999). Sedimentation processes in a tectonically active environment: The Kerkyra-Kefalonia submarine valley system (NE Ionian Sea). *Marine Geology*, 160, 25–44.
- Preka-Alexandri, K. (1986). *Κέρκυρα, Παλαιόπολη* (Corcyra, Palaiopoli). *Archaologikon Deltion*, 41B, 125–129.
- Reimer, P. J., Bard, E., Bayliss, A., Becks, J. W., Blackwell, P. G., Bronk Ramsey, C., ... Van der Plicht, J. (2013). INTCAL13 and MARINE13 radiocarbon age calibration curves 0–50,000 years cal BP. *Radiocarbon*, 55, 1869–1887.
- Reimer, P. J., & McCormac, F. G. (2002). Marine radiocarbon reservoir corrections for the Mediterranean and Aegean Seas. *Radiocarbon*, 44, 159–166.
- Reinhardt, E. G., Goodman, B. N., Boyce, J. I., Lopez, G., Van Hengstum, P., Rink, W. J., ... Raban, A. (2006). The tsunami of 13 December A.D. 115 and the destruction of Herod the Great's harbor at Caesarea Maritima, Israel. *Geology*, 34, 1061–1064.
- Riginos, G., Karamanou, A., Kanta, K., Metallinou, G., & Zernioti, D. (2000). Η Αρχαία Κέρκυρα - Πόλη και Ύπαιθρος - Μέσα από τα πορίσματα των πρόσφατων ερευνών (Ancient Kerkyra—City and rural areas—From the results of the recent investigations). In G. Pentogalos, P. Kalligas, D. Minotos (Ed.), *Στ' Διεθνές Πανιώνιο Συνέδριο* (Proceedings of the, pp. 25–38). Thessaloniki: University Studio Press. *6th International Panionian Conference*.
- Sachpazi, M., Hirn, A., Clément, C., Haslinger, F., Laigle, M., Kissling, E., ... Ansorge, J. (2000). Western Hellenic subduction and Cephalonia transform: Local earthquakes and plate transport and strain. *Tectonophysics*, 319, 301–319.
- Sakuna, D., Szczuciński, W., Feldens, P., Schwarzer, K., & Khokiattiwong, S. (2012). Sedimentary deposits left by the 2004 Indian Ocean tsunami on the inner continental shelf offshore of Khao Lak, Andaman Sea (Thailand). *Earth, Planets and Space*, 64, 931–943.
- Schrott, L. (2015). *Gelände-Arbeitsmethoden in der Geomorphologie*. In F. Ahnert (Ed.), *Einführung in die Geomorphologie*. Stuttgart: Verlag Eugen Ulmer KG.
- Schulmeister, M. K., Butler, J. J., Healey, J. M., Zheng, L., Wysocki, D. A., & McCall, G. W. (2003). Direct-Push electrical conductivity logging for high-resolution hydrostratigraphic characterization. *Ground Water Monitoring & Remediation*, 23(3), 52–62.
- Scicchitano, G., Monaco, C., & Tortorici, L. (2007). Large boulder deposits by tsunami waves along the Ionian coast of south-eastern Sicily (Italy). *Marine Geology*, 238, 75–91.
- Seeliger, M., Bartz, M., Erkul, E., Feuser, S., Kelterbaum, D., Klein, C., ... Brückner, H. (2013). Taken from the sea, reclaimed by the sea: The fate

- of the closed harbour of Elaia, the maritime satellite city of Pergamum (Turkey). *Quaternary International*, 312, 70–83.
- Seeliger, M., Brill, D., Feuser, S., Bartz, M., Erkul, E., Kelterbaum, D., ... Brückner, H. (2014). The purpose and age of underwater walls in the Bay of Elaia of Western Turkey: A multidisciplinary approach. *Geoarchaeology*, 29, 138–155.
- Sen Gupta, B. K. (1999). *Modern foraminifera*. Dordrecht: Kluwer Academic Publisher.
- Shaw, B. (2012). *Active tectonics of the Hellenic subduction zone*. Berlin, Heidelberg: Springer.
- Shaw, B., Ambraseys, N. N., England, P. C., Floyd, M. A., Gorman, G. J., Higham, T. F. G., ... Piggott, M. D. (2008). Eastern Mediterranean tectonics and tsunami hazard inferred from the A.D. 365 earthquake. *Nature Geoscience*, 1(4), 268–276.
- Shennan, I., Long, A. J., Rutherford, M. M., Green, F. M., Innes, J. B., Lloyd, J. M., ... Walker, J. (1996). Tidal marsh stratigraphy, sea-level change and large earthquakes, I: A 5000 year record in Washington, U.S.A. *Quaternary Science Reviews*, 15(10), 1023–1059.
- Shi, S., Dawson, A., & Smith, D. (1995). Coastal sedimentation associated with the December 12th, 1992 tsunami in Flores, Indonesia. *Pure and Applied Geophysics*, 144(3/4), 525–536.
- Siani, G., Paterne, M., Arnold, M., Bard, E., Métivier, B., Tisnerat, N., & Bassinot, F. (2000). Radiocarbon reservoir ages in the Mediterranean Sea and Black Sea. *Radiocarbon*, 42, 271–280.
- Smedile, A., De Martini, P. M., Pantosti, D., Bellucci, L., Del Carlo, P., Gasperini, L., ... Boschi, E. (2011). Possible tsunami signatures from an integrated study in the Augusta Bay offshore (Eastern Sicily–Italy). *Marine Geology*, 281, 1–13.
- Soloviev, S. L., Solovieva, O. N., Go, C. N., Kim, K. S., & Shchetnikov, N. A. (2000). *Tsunamis in the Mediterranean Sea 2000 B.C.–2000 A.D.* Dordrecht: Kluwer Academic Publishers.
- Spetsieri-Choremi, A. (1996). *Das Antike Kerkyra*. Athens: Archaeological Receipts Fund, Ministry of Culture.
- Stiros, S. C., & Blackman, D. J. (2014). Seismic coastal uplift and subsidence in Rhodes Island, Aegean Arc: Evidence from an uplifted ancient harbor. *Tectonophysics*, 611, 114–120.
- Stiros, S. C., Pirazzoli, P. A., Laborel, J., & Laborel-Deguen, F. (1994). The 1953 earthquake in Cephalonia (Western Hellenic Arc): Coastal uplift and halotectonic faulting. *Geophysical Journal International*, 117, 834–49.
- Stock, F., Pint, A., Horejs, B., Ladstätter, S., & Brückner, H. (2013). In search of the harbours: New evidence of Late Roman and Byzantine harbours of Ephesus. *Quaternary International*, 312, 57–69.
- Stucchi, M., Rovida, A., Gomez Capera, A. A., Alexandre, P., Camelbeeck, T., Demircioglu, M. B., ... Giardini, D. (2013). The SHARE European Earthquake Catalogue (SHEEC) 1000–1899. *Journal of Seismology*, 17, 523–544.
- Stuiver, M., & Reimer, P. J. (1993). Extended 14C data base and revised Calib 3.0 14C age calibration program. *Radiocarbon*, 35, 215–230.
- Suric, M., Korbar, T., & Juračić, M. (2014). Tectonic constraints on the late Pleistocene–Holocene relative sea-level change along the north-eastern Adriatic coast (Croatia). *Geomorphology*, 220, 93–103.
- Switzer, A. D., & Jones, B. G. (2008). Large-scale washover sedimentation in a freshwater lagoon from the southeast Australian coast: Sea-level change, tsunami or exceptionally large storm? *Holocene*, 18, 787–803.
- Thucydides after Dent, J. M. (Ed.). (1910). *The Peloponnesian War*. Translated by Richard Crawley. New York: E.P. Dutton.
- van Hinsbergen, D. J. J., van der Meer, D. G., Zachariasse, W. J., & Meulenkamp, J. E. (2006). Deformation of western Greece during Neogene clockwise rotation and collision with Apulia. *International Journal of Earth Science*, 95, 463–490.
- Veerasingam, S., Venkatachalapathy, R., Basavaiah, N., Ramkumar, T., Venkatraman, S., & Deenadayalan, K. (2014). Identification and characterization of tsunami deposits off southeast coast of India from the 2004 Indian Ocean tsunami: Rock magnetic and geochemical approach. *Journal of Earth System Science*, 123, 905–921.
- Véron, A., Goiran, J. P., Morhange, C., Marriner, N., & Empereur, J. Y. (2006). Pollutant lead reveals the pre-Hellenistic occupation and ancient growth of Alexandria, Egypt. *Geophysical Research Letters*, 33, L06409.
- Vött, A. (2007). Silting up Oiniadai's harbours (Achelooos River delta, NW Greece). *Geoarchaeological implications of late Holocene landscape changes. Géomorphologie: Relief, Processus, Environnement*, 1, 19–36.
- Vött, A., Bareth, G., Brückner, H., Curdt, C., Fountoulis, I., Grapmayer, R., ... Willershäuser, T. (2010). Beachrock-type calcarenitic tsunamites along the shores of the eastern Ionian Sea (western Greece)—Case studies from Akarnania, the Ionian Islands and the western Peloponnese. *Zeitschrift für Geomorphologie N.F. Supplementary Issue*, 54(3), 1–50.
- Vött, A., Bareth, G., Brückner, H., Lang, F., Sakellariou, D., Hadler, H., ... Willershäuser, T. (2011a). Olympia's Harbour Site Pheia (Elis, Western Peloponnese, Greece) destroyed by tsunami impact. *Die Erde*, 142, 259–288.
- Vött, A., Brückner, H., May, S. M., Sakellariou, D., Nelle, O., Lang, F., ... Fountoulis, I. (2009). The Lake Voulkaria (Akarnania, NW Greece) palaeoenvironmental archive—A sediment trap for multiple tsunami impact since the mid-Holocene. *Zeitschrift für Geomorphologie N.F. Supplementary Issue*, 53(1), 1–37.
- Vött, A., Fischer, P., Rübke, B. R., Werner, V., Emde, K., Finkler, C., ... Willershäuser, T. (2015). Holocene fan alluviation and terrace formation by repeated tsunami passage at Epitalio near Olympia (Alpheios River valley, Greece). *Zeitschrift für Geomorphologie N.F., Supplementary Issue*, 59(4), 81–123.
- Vött, A., Lang, F., Brückner, H., Gaki-Papanastassiou, K., Maroukian, H., Papanastassiou, D., ... Zander, A. (2011b). Sedimentological and geoarchaeological evidence of multiple tsunamigenic imprint on the Bay of Palairos-Pogonia (Akarnania, NW Greece). *Quaternary International*, 242, 213–239.
- Vött, A., Schriever, A., Handl, M., & Brückner, H. (2007). Holocene palaeogeographies of the central Achelooos River delta (NW Greece) in the vicinity of the ancient seaport Oiniadai. *Geodinamica Acta*, 20, 241–256.
- Walker, M. (2005). *Quaternary dating methods*. Chichester: Wiley.
- Willershäuser, T., Vött, A., Brückner, H., Bareth, G., Nelle, O., Nadeau, M.-J., ... Ntageretzis, K. (2013). Holocene tsunami landfalls along the shores of the inner Gulf of Argostoli (Cefalonia Island, Greece). *Zeitschrift für Geomorphologie N.F. Supplementary Issue*, 57(4), 105–138.
- Yu, K.-F., Zhao, J.-X., Shi, Q., & Meng, Q.-S. (2009). Reconstruction of storm/tsunami records over the last 4000 years using transported coral blocks and lagoon sediments in the southern South China Sea. *Quaternary International*, 195, 128–137.

How to cite this article: Finkler, C, Fischer, P, Baika, K, Rigakou, D, Metallinou, G, Hadler, H, and Vött, A. Tracing the Alkinooos Harbor of ancient Kerkyra, Greece, and reconstructing its paleotsunami history. *Geoarchaeology*. 2017;00:1–19. doi: 10.1002/geo.21609.